

Progress report on the study into the dynamics and growth of ***Ensis directus*** in the near coastal zone off Egmond, in relation to environmental conditions in 2011.

Rob Witbaard, Gerard Duineveld, Magda Bergman

NIOZ Koninklijk Nederlands Instituut voor Zeeonderzoek

Progress report on the study into the dynamics and growth of *Ensis directus* in the near coastal zone off Egmond, in relation to environmental conditions in 2011.

Rob Witbaard, Gerard Duineveld, Magda Bergman

NIOZ, Postbus 59, 1790AB Den Burg Texel

Commissioned by:
Foundation La Mer
Postbus 474
2800 AL Gouda

Colophon

Report number: NIOZ report 2012-7.

Published by: Foundation La Mer.

Referentienummer LM-006588.

Date: February 2012.

Authors: R. Witbaard, G.Duineveld, M.Bergman.

Title: Progress report on the study into the dynamics and growth of *Ensis directus* in the near coastal zone off Egmond, in relation to environmental conditions in 2011.

Project name: La Mer long Deploy.

Commissioned by: Foundation La Mer
Postbus 474
2800 AL Gouda.

Programme: Monitoring and Evaluation Programme Sand mining RWS LaMER, part B5 of the evaluation programme Sand mining (Ellerbroek e.a. 2008).
Monitoring and Evaluation Programme Sand mining Sand engine.

Partners Foundation La Mer
Rijkswaterstaat
Project realization Sand engine.

Supervised by: Marcel Rozemeijer (Imares)
Saa H. Kabuta (RWS-WD)
John de Ronde (Deltares)
Johan de Kok (Deltares)
Rik Duijts (RWS-DNZ)
Evelien van Eijsbergen (RWS-WD)
Sarah Marx (RWS-WD).

Executed by: NIOZ Netherlands Institute for Sea Research
Landsdiep 4
1797 SZ Den Hoorn (Texel).

Availability: After review and approval

Tasks:

Analyses & Reporting	Rob Witbaard, Gerard Duineveld, Magda Bergman.
Lab work organization	Rob Witbaard, Magda Bergman.
Logistics	Rob Witbaard, Magda Bergman.
Lab Work	Hans Witte, Evaline van Weerlee, Joost van der Hoek.
Field work	Crew Terschelling, Rob Witbaard, Gerard Duineveld, Magda Bergman, Hans Witte, Job ten Horn, Evaline van Weerlee, Carola van der Hout, Selma Ubbels, Charlotte Soul, Joost van der Hoek, Roald ter Heide.
Project management	Rob Witbaard, Magda Bergman.

To be quoted as: Witbaard R., G.C.A. Duineveld & M. Bergman (2012). Progress report on the study into the dynamics and growth of *Ensis directus* in the near coastal zone off Egmond, in relation to environmental conditions in 2011. NIOZ report 2012-7.

1. INTRODUCTION

Continuous efforts to protect the Dutch coastline from erosion require large amounts of sand to be annually supplied onto the coastline (year 2010: > 12 million M³). Traditionally sand is supplied on to the beaches but since 1997 beach nourishment is alternated with underwater replenishment at the shoreface. With latter method large amounts of sand are dumped in front of the beach. Apart from the fact that this method is logistically less complex, it also aims at a promotion of the natural processes to reinforce the beach and dunes.
In the meantime a large portion of the coastal zone has been designated as an area of conservation in the framework of inter- and national agreements (NATURA 2000, Natuurbeschermingswet, http://www.noordzeenatura2000.nl/), because of its ecological value for birds and fish. Especially the abundant bivalves form a basic food source of overwintering birds. Over the past 15 years, a doubling has taken place in the total standing stock of bivalves in the Dutch coastal zone. While in the 1990's, *Spisula subtruncata* was the most abundant species occurring in dense aggregations, nowadays the invasive American razor shell, *Ensis directus*, dominates the biomass (Figure 1)(Goudswaard et al, 2011).

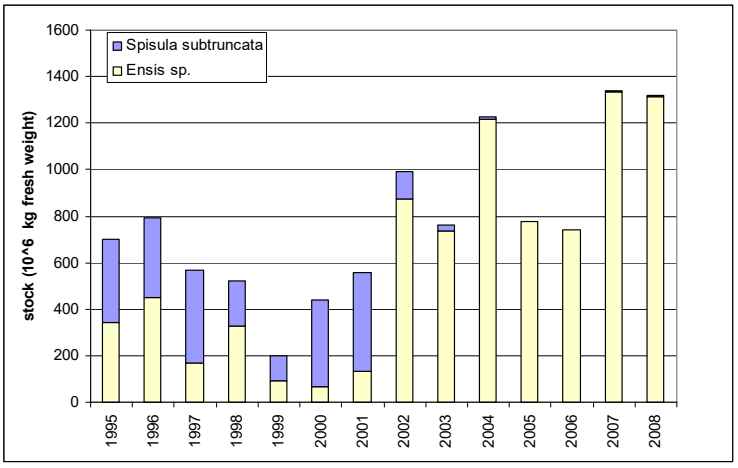

Figure 1. Standing stock of Spisula subtruncata and Ensis directus in the Dutch coastal waters in the period 1995-2008 based on yearly stock assessments with modified hydraulic dredge or trawled dredge; sampling efficiency for *E. directus* is estimated at 50%) (Goudswaard et al, 2008).

The presently known standing stock of *Ensis directus* is substantially higher than previously reported estimates of bivalve biomass. Because *E. directus* rapidly retracts itself deep in the sediment, accurate density estimates are difficult. Moreover a significant number of *E. directus* lives in the shallow shoreface at depths which are difficult to access with ships which can use gear to sample this species quantitatively. Densities are, therefore, likely even higher (Figure 2).

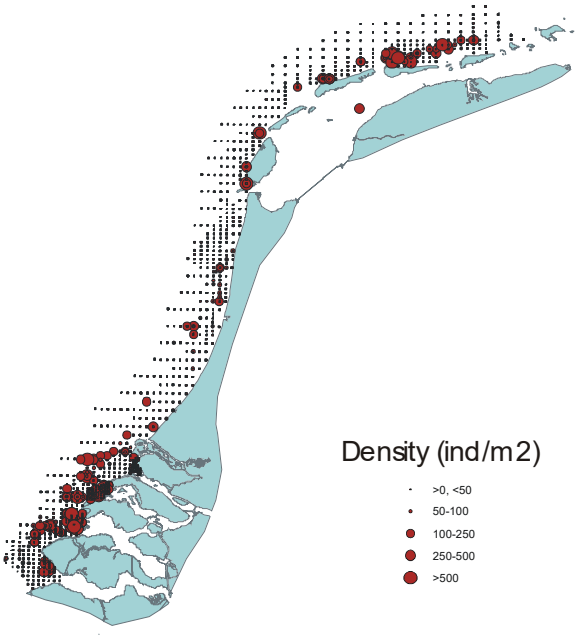

Figure 2. Spatial distribution and density (ind/m²) of *Ensis* sp. in the Dutch coastal waters in the period 1995-2008 based on yearly stock assessments with modified hydraulic dredge or trawled dredge; densities not corrected for 50% sampling efficiency)(Goudswaard et al, 2008).

Shoreface depostion of sand can directly harm bottom organisms that are normally dependent on contact with the overlying water (worms, bivalves) though some species survive burial to some extent (polychaete *Lanice*). With the sand, a small percentage of silt is released. Percentages silt in sediment off the coast vary between 0 and ~4%. Tides transport this material and thereby potentially cause an effect over a larger area than the dumping plot (e.g van Duin e.a., 2007).This in contrast to underwater shoreface replenishements which is likely to have a significant effect on a local scale because of burial and smothering of the original bottom surface with it's fauna.

In chapter 6 of the evaluation program of the MER (Ellerbroek et al, 2008) several knowledge gaps which were identified and outlined. These deal with the distribution of SPM (Suspended matter),negative "Far field" effects of increased SPM concentrations on primary production and effects of the increase of SPM in relation to natural conditions as well as its effect on the disturbance of spatial and temporal distribution of species. In more detail the Monitoring programme RWS LaMER research program focuses on:

(1) What are the effects of the reduced food conditions on the growth of *E. directus*
(2) When does food limitation occur as a result of these changed conditions?

Many filter-feeding invertebrates (bivalves and polychaetes) show a depressed filtration activity and growth rate in the presence of large concentrations of suspended silt (Wilber and Clarke 2001, Archamboult et al 2006). The bivalve species inhabiting the Dutch coastal zone (e.g. *Ensis directus*, *Macoma baltica*, *Tellina tenuis*) have to cope with natural high concentrations of silt. Longshore SPM transport in a narrow strip along the Dutch coast (Anonymous, 2002) is estimated to be in the order of 10 to 20 million tons per year (Van Alphen, 1990; De Kok, 2004) but this is most likely an underestimate. Nevertheless, preliminary laboratory experiments showed that *Ensis directus* show depressed clearance rates under high silt concentrations (Witbaard & Kamermans 2011).

Thus, as *Ensis directus* nowadays plays an important ecological role in the coastal “protected” zone more insight into determinants of the feeding behaviour and growth of this species is especially important to assess and validate effects of increased SPM concentrations caused by shoreface and beach nourishment or sand extraction elsewhere.
To obtain such insights, we deployed a measurement platform (lander) at 10m water depth off Egmond equipped with a sensor package (turbidity, chlorophyll, T, S, current) and a monitor recording the gape of multiple individuals of two bivalve species (*Ensis directus*, *Mytilus edulis*). More specifically we asked the following questions in this particular study:

1. What is the natural variation in silt concentrations close to the seabed
2. What is the forcing factor of this variation (erosion, advection, season)
3. Is the valve gape of *Ensis* related to the silt concentration and how (linear, stepwise) if not which other factors control the gape of *Ensis*.
4. What factors are most important determinants of the growth of *Ensis directus*

The research and results presented here consists of two parts. The first part deals with assessment of natural variation in environmental conditions close to the seafloor continuously measured with abovementioned autonomous measurement (lander) platform. The second part deals with *in situ* sampling of the local *Ensis directus* population with the aim to follow timing of growth, reproduction and follow population development.
In the end, the data obtained from this field monitoring off shore Egmond (2010, 2011 and 2012) will be used to develop, calibrate and validate a DEB (Dynamic Energy Budget) model for *E. directus* (Wijsman e.a., 2011, Kamermans e.a. 2011, Cardoso e.a. 2011, Cardoso e.a., 2006,Cardoso e.a. 2009).
As a next step, the integration of the DEB model into the Delft 3D (e.g. Schellekens 2012) water quality model will provide a useful management tool to assess the effects of beach nourishments and sand extraction on the level of individual organisms and populations and the potential effects on secondary production by *Ensis directus*. This latter work is now in progress.

This research represents the results of section B5 of the evaluation programme of Ellerbroek e.a. (2008). The Monitoring and Evaluation Programme Sand mining Sand engine participates in this programme to fulfil their monitoring requirements on monitoring the impact of sand mining on silt and the impact of extra silt and reduced food conditions on the growth of *E. directus.*

This literature mentioned in this report by far not covers all aspects of the research field, nor does this report give a literature review. Because of time limitations, we focussed on the presentation and interpretation of the results obtained exclusively within the project itself, without relating it to results reported in literature.

2. METHODS

Lander Deployments

At about one kilometer off the coast of Egmond a lander platform was placed at a depth of 11 meter (Figure 3, table 1).

Table 1. Positions of and around the central lander position at where boxcore samples are taken to follow the seasonal development of sediment grain size and to follow the wax and wane of the local *Ensis* population.

station	gr min dec min N	gr min dec min E	gr dec gr N	gr dec gr E
LNE (Lander North East)	52° 38.28'	4° 36.356'	52.6380°	4.605933°
LSE (Lander South East)	52° 38.216'	4° 36.380'	52.6369°	4.606333°
LSW (Lander South West)	52° 38.22'	4° 36.22'	52.6370°	4.603667°
LNW (Lander North West)	52° 38.281'	4° 36.22'	52.6380°	4.603667°
Lander	52° 38.249'	4° 36.294'	52.63748°	4.6049°

Figure 3. Location of the lander station and the four stations around this location at which additional sampling takes place. Distance from the lander to the beach is approximately 1 km. Egmond is situated in the south east corner of the map (not visible). The depth of the location is approximately 11 meter.

The lander platform consists of an triangular aluminium frame (Height Width: 2 x 2 m) with a series ballast weights (total 500 kg) fixed onto the lower support that stands on the seafloor. In this way the center of gravity is lowered as much as possible preventing the platform from falling over during storms. On top of the platform is a pop-up system with a 50-m rope connected to 40 kg floatation. The pop-up is triggered from the surface by 2 acoustic releasers (http://www.ixsea.com/). The platform carries 1 closeable mesocosm. This mesocosm is opened (and closed) by means sliding top valves activated with hydraulics. The hydraulics are operated by an ALTRAP pump (Fig. 4).

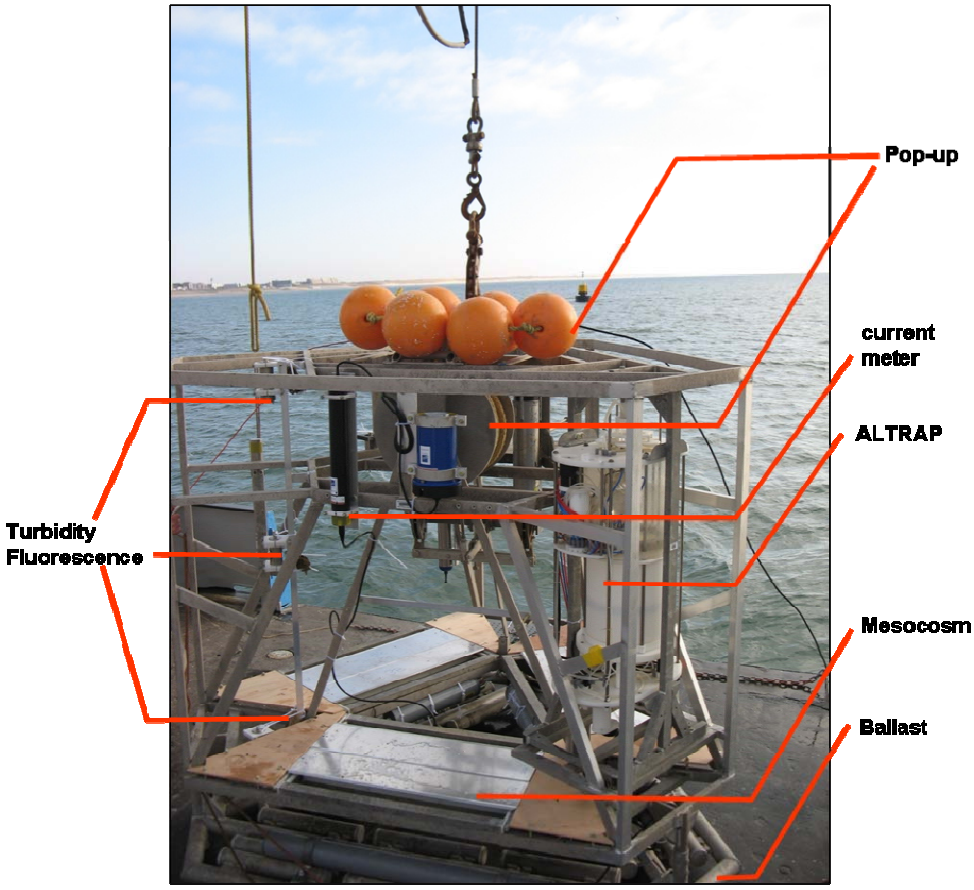

Figure 4. Overview of one the lander frames used in the environmental monitoring off the coast of Egmond in 2011.

Before deployment of the lander, the mesocosms are closed this to prevent sediment to be washed out from the containers carrying live *Ensis*. At planned end of the deployment the mesocosm is kept open as sediment loss at this moment is not important as valve gape monitoring will be stopped once the lander comes on deck.

The platform carried 2 gape monitors. Each monitor is simultaneously measuring the gape of 7 bivalves with a frequency of 1/60 Hz (T=0.016 $s^{-1)}$. The gape size is measured by means of the inductive current generated through a pair of micro-coils which are glued to the valves (Fig. 5). One gape monitor was connected to 7 Mussels (*Mytilus edulis*) that were attached to the underside of a PVC plate (Fig. 5). The PVC plate was bolted onto the platform at 30 cm above the sediment. The second gape monitor was connected to 7 specimens of *Ensis directus* that were contained in sand filled cylinders in one of the mesocosms (Fig. 6). Both gape monitors had one blank sensor to be used as a control signal.

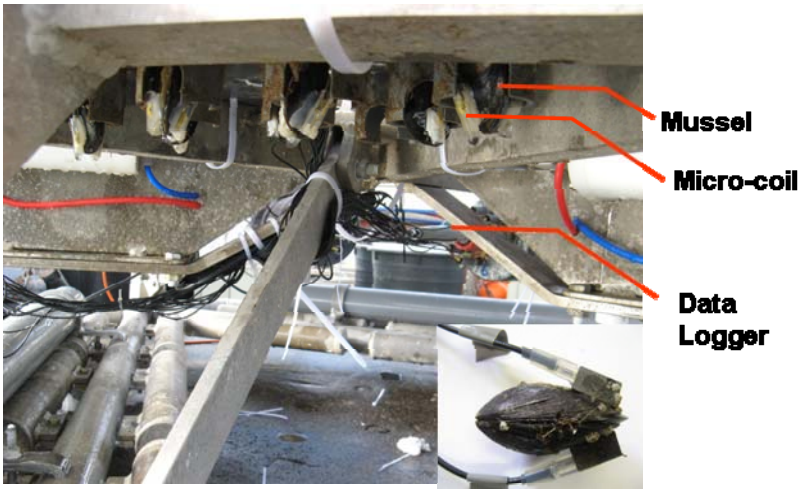

Figure 5. Detail picture of the valve monitor with attached mussels, hanging at 30 cm above the seafloor. Mussels pointing down wards in half open cups in which they can attach themselves.

Figure 6. Placement of sediment cores with live *Ensis* connected to a valve monitor in one of the trays which are mounted on the lander.

The lander platform was furthermore equipped with a series of sensors measuring the following physical parameters: current, temperature, salinity, turbidity and fluorescence. Current speed and direction (3D) were measured every 10 min at 140 cm above the bottom with a NORTEK aquadopp Doppler current meter. This instrument also yielded a record of the acoustic backscatter. Temperature and Salinity were measured every 10 min with a pumped version of the Seabird SM37 CTD system (http://www.seabird.com/). The CTD sensors are protected from effects of fouling by the presence of a TBT impregnated plastic ring inside the dead volume of the pump.

In addition to the NORTEK aquadopp current meter a NORTEK Vektor current meter (http://www.nortek-as.com/) was mounted at the lander at a height of 30 cm above the bottom. Every 10 minutes this instruments made high frequency burst measurements during 2 minutes with a frequency of 1. Deltares takes care of detailed analyses of these Vektor data. Sensor “glasses” from both the Vektor and aquadopp current meters were protected against fouling by applying a light veneer of udder ointment.

Turbidity and fluorescence were measured optically at four heights above the bottom, i.e. 30, 80, 140 and 200 cm, using ALEC Compact-CLW's (http://ocean.jfe-advantech.co.jp) with wipers to keep fouling under control. The measurement at the lowest height (30cm) was done with the infinity version of the instrument as it can deal with higher turbidity. The wiped versions appeared all to be crucial for obtaining optic records in coastal environments with heavy fouling. All Alec sensors have been calibrated in the lab over a range of local SPM and chlorophyll concentrations. In this report we refer to the material being measured as turbidity as SPM. The fluorescent part of it, and simultenously measured is referred to as Chlorophyll.
During three deployment periods (May 3-31, June24-July12, Oct 25-Jan 11.) Deltares placed a LISST 100 (http://www.sequoiasci.com/) upon the lander frame to measure the particle size distribution of suspended material.

The platform was launched on 22/Feb/2011 with the RV Terschelling (RWS) (Figure 7). The position of the platform was marked by two buoys protecting it from trawling activity. In table 2 an overview of the deployment and retrieval dates is given.
Table 2. Overview of deployment dates and ships used in 2011.

Deployment nr/period		Date	Ship
1	week 08	22/02/2011	Terschelling
2	week 14	07/04/2011	Terschelling
3	week 18	03/05/2011	Terschelling
4	week 22	31/05/2011	Terschelling
5	week 25	24/06/2011	Pelagia
6	week 28	12/07/2011	Terschelling
7	week 31	02/08/2011	Terschelling
8	week 34	23/08/2011	Terschelling
9	week 39	27-28/09/2011	Terschelling/Pelagia
10	week 43	25/10/2011	Terschelling
11	week 02	11/01/2012	Terschelling

Figure 7. . Deployment of one of the lander platforms off the coast of Egmond.

In spring and autumn the platform is retrieved for maintenance and data collection every 5th or 6th week. During the summer the platform is retrieved every third week to prevent problems and minimize the effects of fouling by barnacles and other epifaunal organisms. For most of these 1 day maintenance cruises the RWS ship Terschelling has been used. This with the exception of two times when RV Pelagia had been used for these operations (24th June & 27th September 2011) (See table 2)

Valvometry

During every deployment period two valve monitors were mounted on the lander frame. The first valve monitor hosted 7 live mussels (*Mytilus edulis*) (Figure 5), the second valve monitor hosted 7 *Ensis directus* (Figure 6). The average start size of the mussels was 39 mm and the size of the *Ensis directus* used was approximately 115 mm. Of each bivalve the valves were attached to sensors on basis of which the relative gape distance could be measured and monitored. Measurement frequency in both instances was 1/minute (T=0.016). Of each valve monitor the 8th channel was used as control on the electronics, i.e. no bivalve was attached. The experimental *Mytilus edulis* were hang in cavities at the underside of a pvc plate which on its turn was mounted on the lander. This was done to prevent the accumulation of sedimenting mud and sand which could smother the animals. The *Ensis* were placed in pvc tubes which were hosted in a tray like construction. During deployment of the lander this tray was closed with a lid which would open at a pre-programmed time i.e. once the lander was on the seafloor. This was done to prevent that the substratum in the tubes which hosted the *Ensis* was being washed out. The height at which both valve monitors were placed on to the lander was within the measuring range of the lowest placed turbidity sensor, i.e. 30-45 cm. As far as possible, the same animals were used again in following deployment periods.

Additional sampling

During each service operation two boxcore samples at each of the four corner locations around the (central) lander platform position were taken (see table 1; LSE,LSW,LNE,LNW). If the boxcore sample was of sufficient quality a subcore for sediment grain size analyses was preserved. These samples have been split into two layers of 5 cm height and kept frozen until freeze dried. The remainder of the boxcore was sieved over a 1 mm screen and the live *Ensis* were collected and stored for size measurements and ash free dry weight (AFDW) determination. In this way a time series of the growth and population development of the local *Ensis* stock is obtained on basis of population averages.
In addition to these samples additional boxcores were taken to collect at least 50 *Ensis* individuals for determination of the seasonal change in gonado-somatic index and change in glycogen and energy reserve content. On board all samples were stored refrigerated.

Lab procedures

Population development and average individual growth.

To determine seasonality of shell growth, tissue growth and gonad development the *Ensis* population around the lander was followed by collecting the living animals from (additional) boxcore samples taken at the four stations around the lander taken at each of sampling dates. All living animals were routinely measured with digital callipers. Three measurements were made, length, width and thickness. Together with these size measurements the ash free dry weight was determined in the lab. For this, the soft tissue was removed, dried at 60°C until constant weight and then incinerated at 540°C during 4 hours. The weight difference of dry weight and ash-weight is the ash free dry weight.

Weights-Gonado somatic index.

In addition to above sampling extra individuals were collected. In the lab a selection of 50 individual of different size classes from the entire size range was made. From these animals the shell size (length, width and thickness) were measured as well as their wet weights. There after gonads were separated from the somatic tissue and after drying both fractions were incinerated to obtain the ash free dry weights of these tissues. These weights were used to calculate the contribution of the gonadal mass in the total weight of the animals. Based on these determinations and the collection of data over the seasons, the change in gonadal mass over the season could be determined.

Glycogen analyses / Caloric content.

Not yet performed but in progress.

3. Results.

Ensis directus

For the period up to 11/01/2012 the mean density of *Ensis directus* around the lander is 184 individuals/m². The variation between samples taken at different sites, stations and dates is large (Table 3). The average densities at the southern stations (LSW and LSE) seem to be higher than at the northern stations but the only statistical difference in density could be detected between station LSW and both Northern stations (LNW and LNE).

Table 3. The average densities per station (n/m²) and sampling date are given. Only the density at station LSW differs significantly from both northern station (LNW –LNE). The other observed density differences between the stations are not significant. (Tukey HSD pairwise comparison, $p<0.05$).Letter codes refer to sampling locations around lander. LNW=lander North West, LSW=Lander South West, LNE=Lander North East, LSE=Lander south East. Avg=Average, Stdev=Standard deviation.

Date/Station	**LNW**	**LSW**	**LNE**	**LSE**	**Avg**	**Stdev**
22/02/2011	147.2	582.4	121.6	441.6	323	226
07/04/2011	236.8	313.6	179.2	320	262	67
03/05/2011	108.8	70.4	64	108.8	88	24
31/05/2011	76.8	313.6	428.8	224	261	149
24/06/2011	140.8	83.2	64	147.2	109	41
12/07/2011	76.8	243.2	172.8	166.4	165	68
02/08/2011	134.4	524.8	102.4	185.6	237	195
23/08/2011	185.6	185.6	211.2	147.2	182	26
28/09/2011	153.6	307.2	121.6	185.6	192	81
25/10/2011	134.4	64	70.4	76.8	86	32
11/01/2012	70.4	121.6	128	147.2	117	33
Average	133	255	151	195	184	86
Stdev	50	177	104	103	80	71

This density difference coincides with a size difference between stations. This is illustrated in the notched box and whisker plot (Figure 8) which illustrates this size difference as non overlapping notches between the subsequent stations. This statistical difference is confirmed in a Tukey HSD pair wise comparison ($p<0.05$). The small difference is not taken into further account as the mean of the pooled stations is regarded to reflect a regional average for the area around the lander.

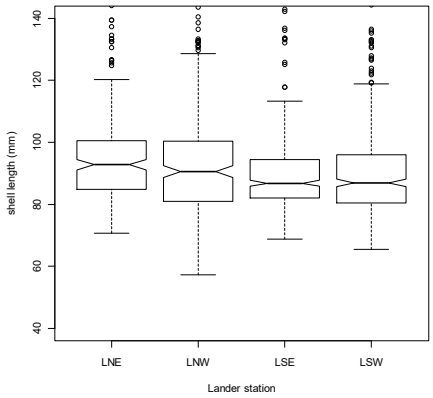

Figure 8. Notched Box and whisker plot of the shell lengths *Ensis* collected from the four stations around the central lander position. Non overlapping notches implies that there is a statistical significant difference in shell sizes showing that the average size at the southern stations are slightly smaller than at the northern stations.

The *Ensis* population collected at the four stations around the lander has a bimodal size distribution as depicted in figure 9. Most abundant animals have sizes of approximately 80 mm shell length and around 130 mm shell length. The first category is a cohort which has settled in 2009. The other group is an accumulation of different aged animals which had settled before 2009.

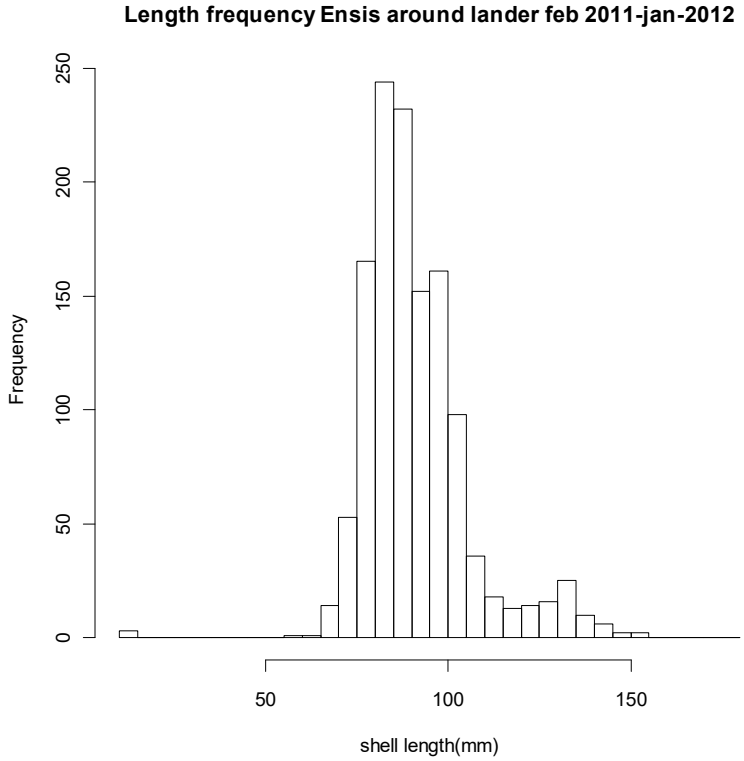

Figure 9. The average size distribution of *Ensis directus* around the central lander station as determined from samples collected between February 2011 and January 2012.

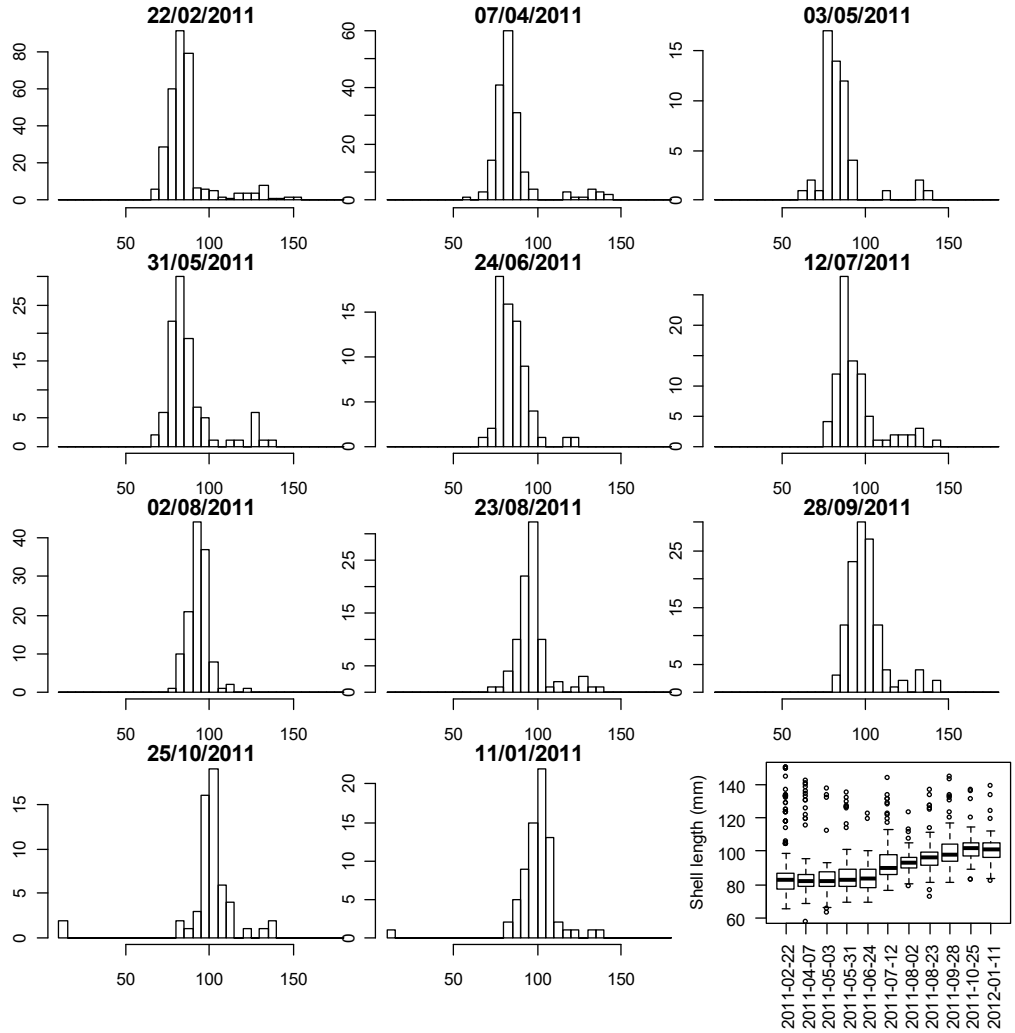

Figure 10. Size distribution of *Ensis* derived from samples which were pooled by collection date and location (Station), together with a boxplot giving an overview of the change in shell length over time.

The pooled collection of samples taken around the lander at each sampling occasion (n=8) is used to estimate shell growth over time in the field. Figure 10 &11 suggests that there is hardly any increase of shell lengths up to the end of June. Between June 24th and the July 12th the first significant shell growth took place. The notched box and whisker plot of those *Ensis* which had lengths smaller than 110mm, which limits the results to the cohort which had settled in 2009, (Figure 11) suggests that the observed length increase is statistically significant.

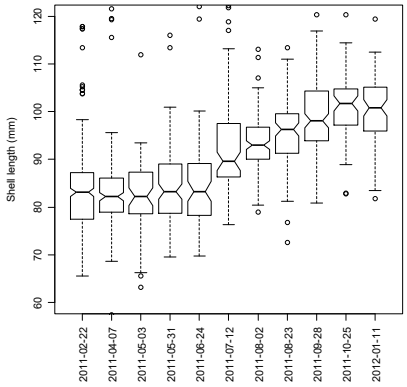

Figure 11. Notched box and whisker plot giving the shell length for each measurement date. Up to June 24th no statistical significant difference appears in shell length. After that that a gradual increase and often statistical significant shell growth took place. Statistical differences are visible as non overlapping notches.

Weight change

In Figure 12 the ash free dry weights of all animals collected for the somatic gonadal index (50 each date) is given. In figure 13 ash free dry weights of exclusively animals belonging to the smaller sized cohort (<110 mm, settled since 2009) is depicted. Both graphs illustrate an jump wise increase in the Ash free dry weights between April 7th and May 3rd. This rapid increase coincides with the spring phytoplankton bloom.

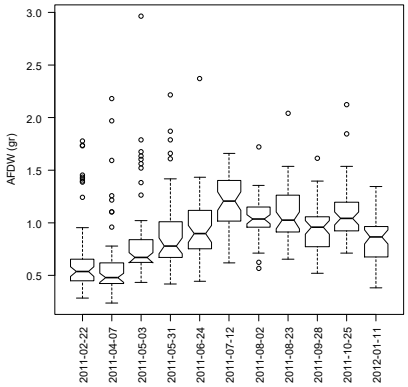

Figure 12. . Ash free dry weight of all collected *Ensis* which were collected around the lander location. Weights are given as notched boxplots by collection date. Non-overlapping notches imply a statistical significant difference in weight between the corresponding dates.

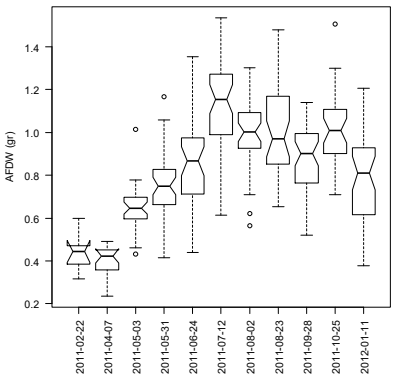

Figure 13. . Ash free dry weights of *Ensis* (which settled since 2009 with shell sizes less than 110 mm) collected around the lander location. Weights are given as notched boxplots by collection date. Non-overlapping notches imply a statistical significant difference in weight between the corresponding dates.

Because the AFDW as depicted in figures 12 and 13 show the increase in bodyweights related to increasing shell lengths, the size corrected weights, expressed as condition index were determined as well. These are depicted in figure 14.

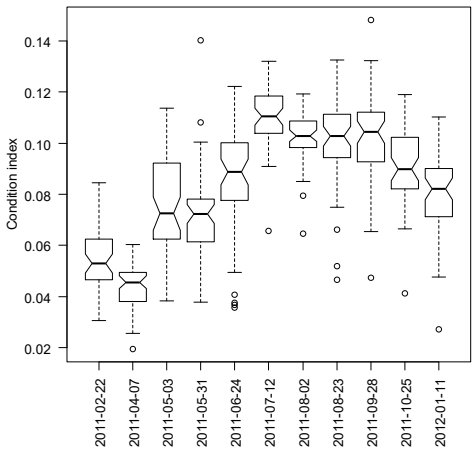

Figure 14. Condition index of *Ensis directus* at the four stations around the lander over time.

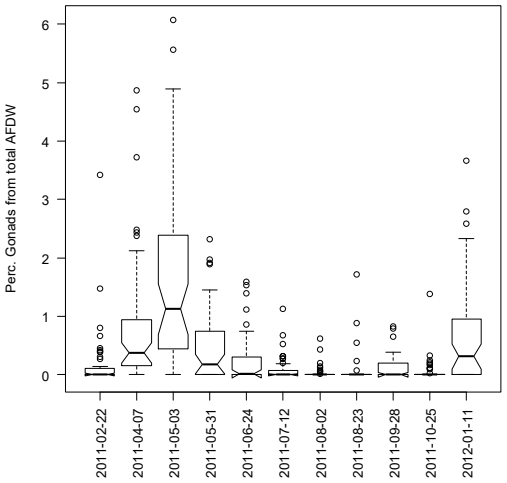

Figure 15. Percentage of gonadal tissue of *Ensis directus* over time.

There is an increase of the condition index between April and June. The increase is greatest in spring. The best condition is found in the summer months. After mid July condition indices tend to decrease. The increase of the condition index between collection dates are significant as is suggested by the limited overlap of the notched box and whisker plots. The suggested decrease since July 12th is insignificant. In Figure 15 the percentage of gonad tissue of the total ash free dry weight is given. The largest percentage was found in the beginning of May. In this period 90 % of the dissected specimens had developed gonads. Bigger and heavier animals tend to have relatively smaller amounts of gonadal tissue but in absolute terms the bigger animals have larger gonadal masses (Figure 16). Over the entire period from 229 specimens the sex could be determined. The sex ratio was almost 1. No differences between sexes in terms of shell length, total AFDW or gonadal AFDW has been observed.

A combination of the data of shell growth and change in Ash Free Dry Weights is given in figure 17. In summary, in early spring the gonadal development starts. After spawning the growth of somatic tissue takes over subsequently followed by shell growth starts. As such growth is divided in different phases.

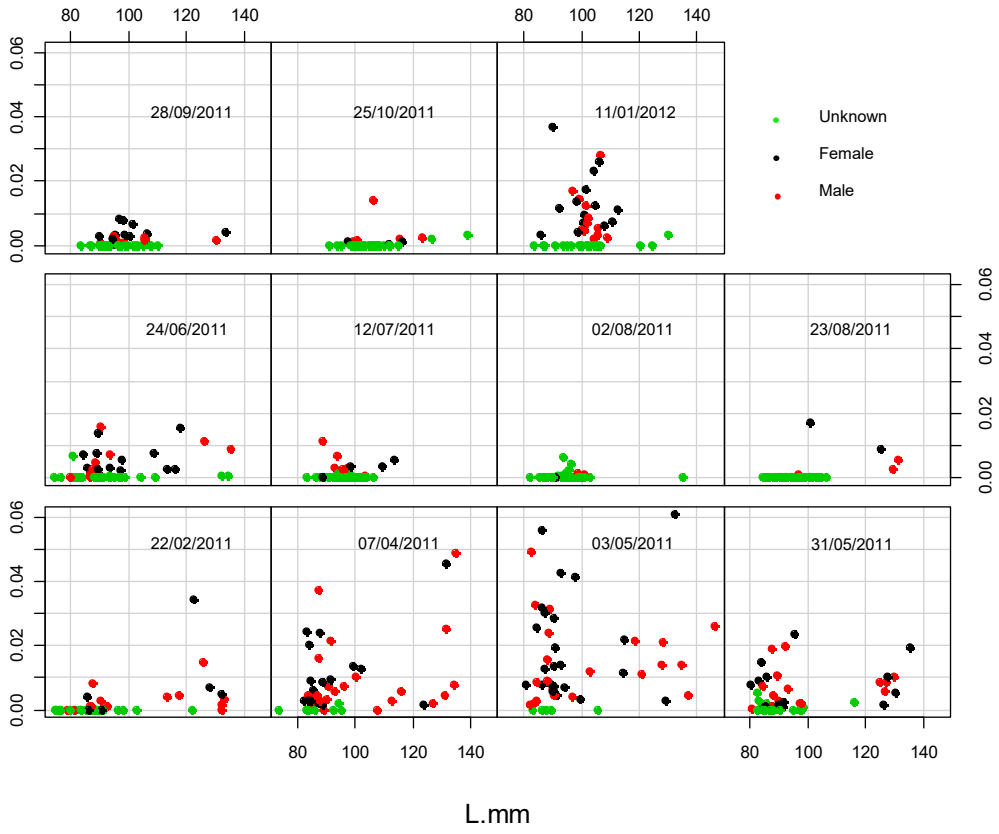

Figure 16. Size dependent fraction of Gonadal Tissue from the total AFDW for animals collected in 2011 around the lander platform. For every period 50 individuals were dissected.

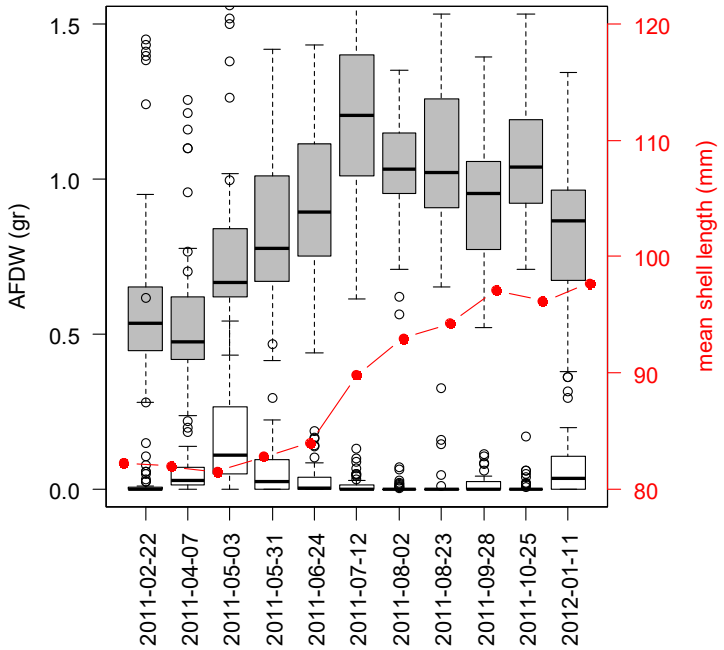

Figure 17. A combination plot of the seasonal change in ash free dry weights of the somatic tissue (grey boxplots), gonadal tissue (white boxplots and of the average length of *Ensis directus* collected around the lander location and which had settled in 2009. (shell lengths smaller then 110m) (red line).

Environmental Data.

Temperature and Salinity

Figure 18 gives the temperature and salinity measured at 10 minute intervals over the entire experimental period. Temperature ranged between 3.9 and 18.6 deg °C. Salinity ranged between 28 and 32 ‰ . Both parameters show a well defined tidal cycle (Fig 19) which is present all through the measurement period. The summary table (Table 4) shows the abiotic conditions in terms of these two parameters are rather constant despite the near coastal environment. There seems to exist a salinity minimum in spring and autumn but the amplitude of this seasonal mean is of the same order of magnitude as the variation in salinity over a tidal cycle (Figure 18). In December 2011 the CTD stopped working halfway the deployment period. Hence no data are available towards the end of 2011. The data also show that there is an effect of the spring – neap tide tidal cycle.

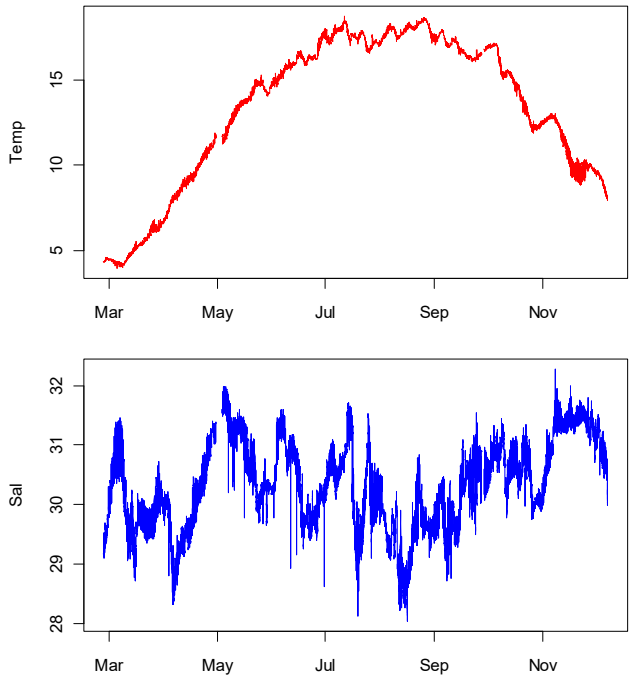

Figure 18. Salinity and temperature record up to 11 January 2012 off the coast of Egmond with a local waterdepth of 11 meter. Measurements are made at an height of 140cm above the bottom.

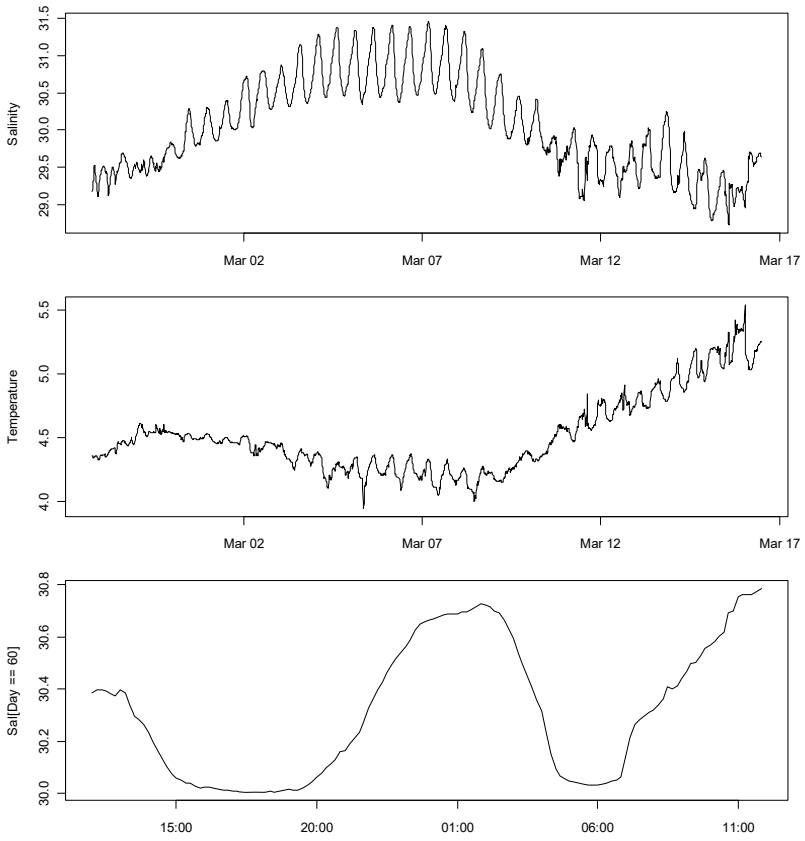

Figure 19. Illustration of the tidal changes in salinity and temperature at the lander location in spring. Showing that there is a spring neap tide cycle in the salinity as well as an effect of the daily tidal cycle.

Table 4. Monthly means and standard deviation of temperature (°C) and salinity (‰) at the lander location near Egmond at 11 meter depth in 2011.

	Temp.	sdev	Sal	sdev
Month	°C.	Temp	ppt	Sal.
Feb	4.48	0.07	29.62	0.25
March	5.24	0.83	29.99	0.53
April	9.31	1.3	29.94	0.73
May	13.63	1.02	30.86	0.58
June	16.03	0.71	30.41	0.58
July	17.57	0.41	30.43	0.54
Aug	17.91	0.35	29.47	0.5
Sept	16.89	0.5	30.13	0.51
Oct.	14.58	1.67	30.57	0.38
Nov	11.00	1.32	31.27	0.36
1-7 Dec	9.02	0.52	30.94	0.29

Currents.

Table 5 gives key values for the current velocities in m/s. in each month and Figure 20 summarizes the measured current data by month as a series of vector plots.
It is obvious that in 2011 the residual current regularly had a southerly direction. In April this reverses and residual current gets a northward direction.

Maximum current speeds of over 1 m/s were measured during a storm in September. Figure 21 gives a contour plot over time, based on the current measurements made at 30cm above the seafloor and those made at 140cm above the seafloor. Features visible are the spring neap tide cycle as well as increased current speeds which penetrate the entire watercollumn up to the bottom.

Table 5. Key values (speed in m/s) of the current vector measured at 140 cm above the seafloor. Given are minimum and maximum and current components as well as the average in each month.

Month	Min North	Max North	Avg North	Min East	Max East	Avg East	Min Up	Max Up	Avg Up
Feb'11	-0.52	0.328	-0.089	-0.126	0.115	-0.020	-0.135	0.223	0.013
March	-0.549	0.487	-0.060	-0.209	0.111	-0.024	-0.155	0.305	0.025
April	-0.461	0.718	0.021	-0.137	0.166	-0.003	-0.144	0.356	0.037
May	-0.566	0.827	0.041	-0.12	0.188	0.021	-0.129	0.217	0.004
June	-0.532	0.566	-0.014	-0.191	0.413	0.056	-0.159	0.489	0.067
July	-0.646	0.757	-0.016	-0.233	0.25	-0.006	-0.168	0.394	0.048
Aug	-0.601	0.828	0.030	-0.206	0.35	0.018	-0.164	0.405	0.043
Sept	-0.558	1.213	0.068	-0.126	0.231	0.030	-0.134	0.373	0.026
Oct	-0.698	0.972	0.020	-0.251	0.214	0.022	-0.132	0.233	0.006
Nov	-0.731	0.773	-0.002	-0.161	0.334	0.023	-0.152	0.374	0.007
Dec	-0.744	1.031	-0.004	-0.497	0.418	0.035	-0.291	0.633	0.063
Jan ‘12	-0.719	0.99	-0.007	-0.403	0.433	-0.005	-0.249	0.834	0.049

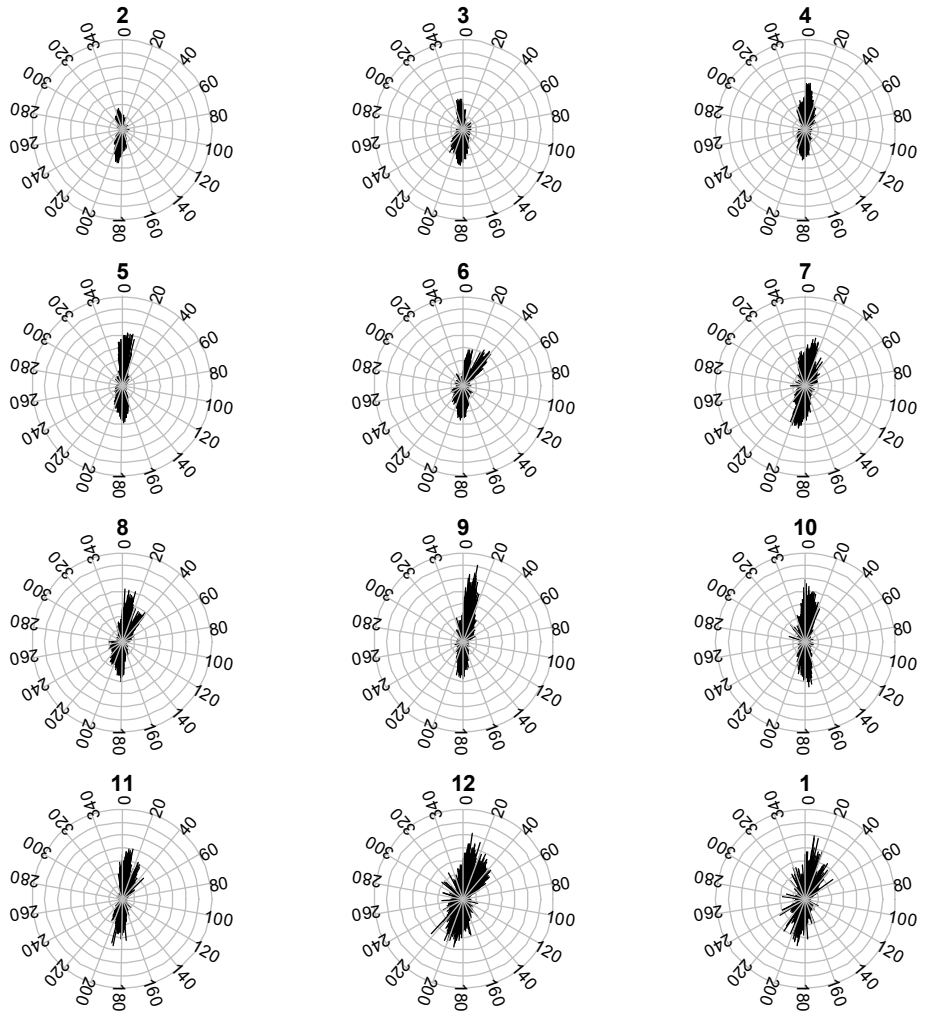

Figure 20. Vector plots of current direction and strength by month (month 2 '11 to 01-2012) . Months indicated as number on top of each radial plot. Radial grid steps reflects current speed in steps of 0.2 m/s. Outer circle is maximum speed of 1.4 m/s. Labels around outer circle is current direction in degrees.

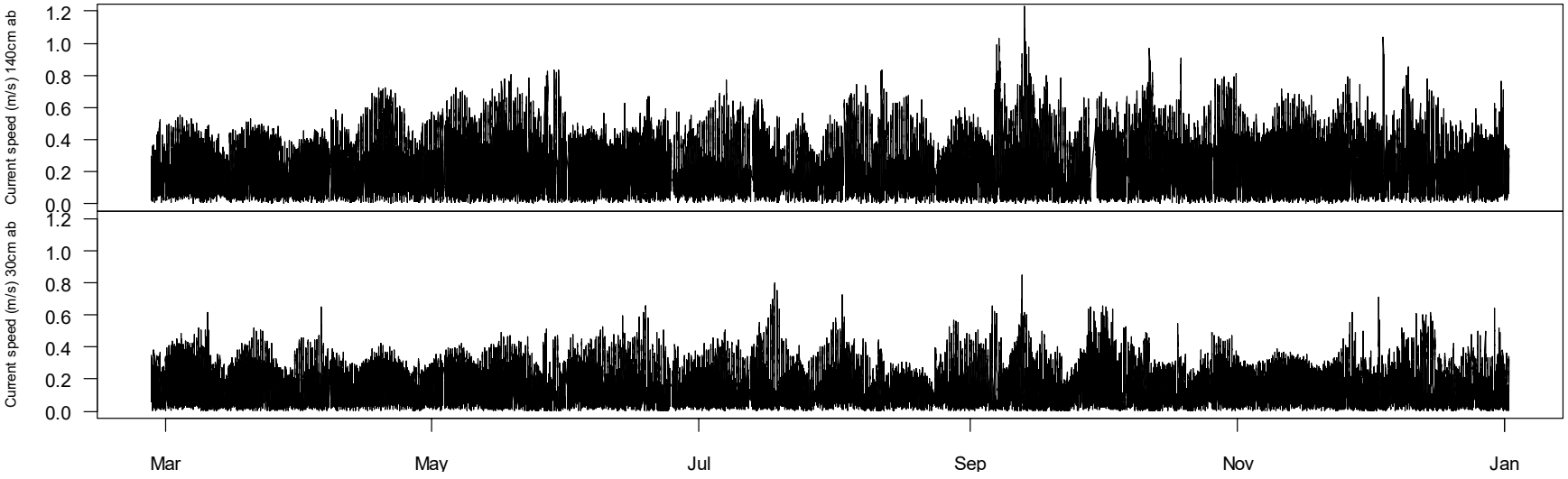

Figure 21. Contour plot of the current speed measurements at 30cm height (Vektor) and those made at 140 cm above the seafloor (Aquadopp) Speed in m/s.

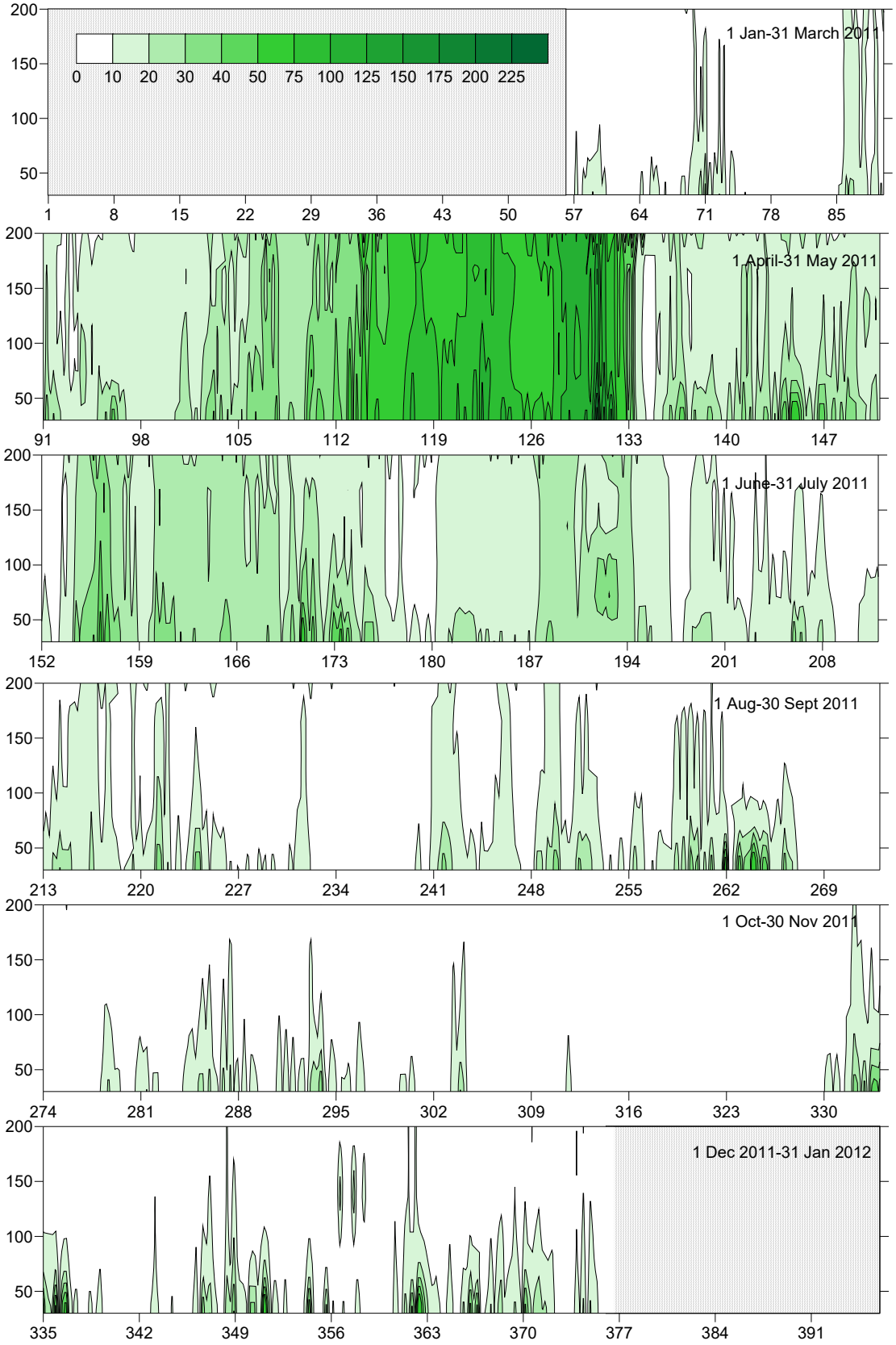

Figure 22. Contourplots of chlorophyll-a concentrations over the measurement period. Numbers along x-axis is day number since 1/1/2011. Numbers along y axis denote height above the seafloor.

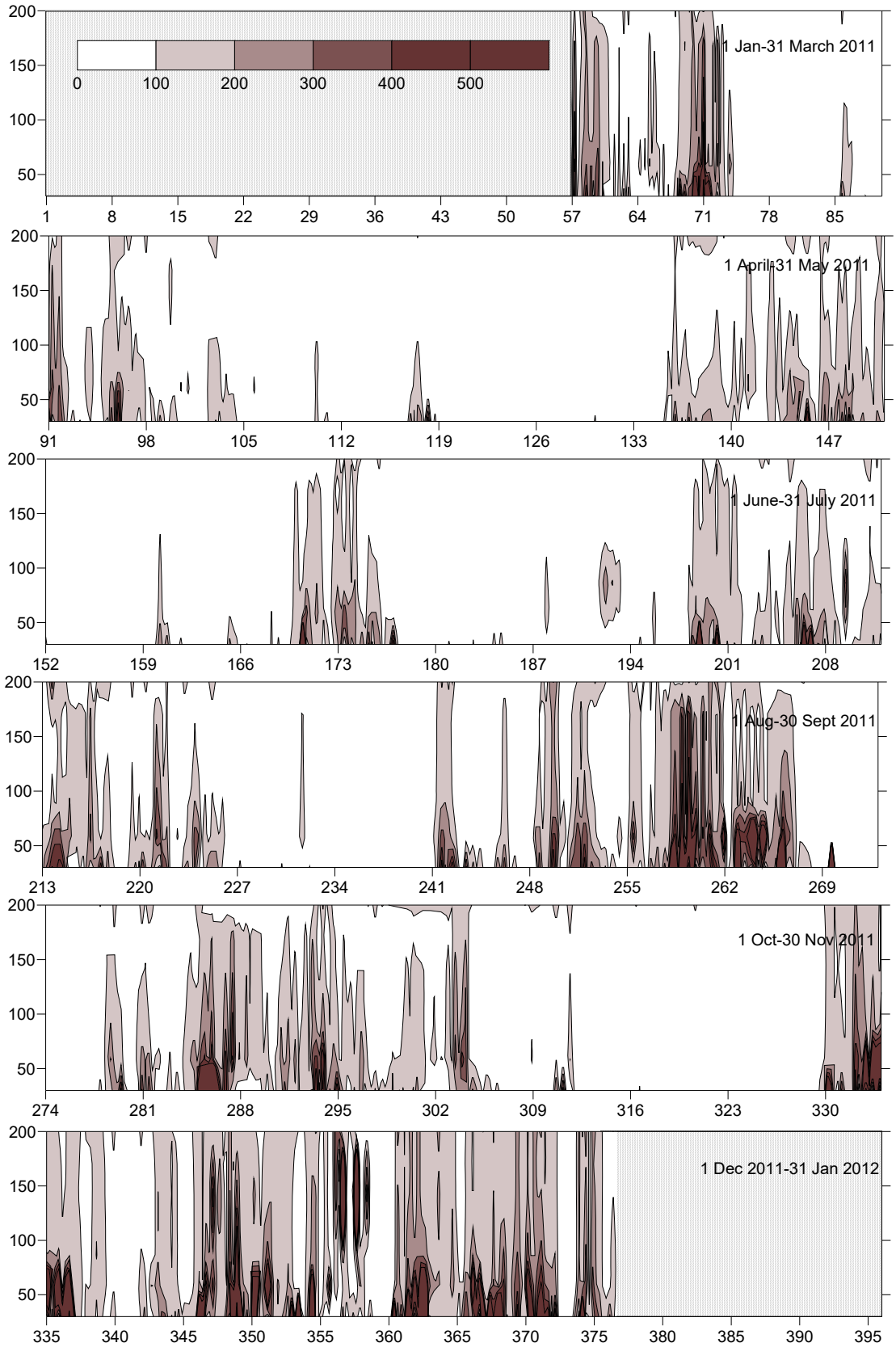

Figure 23. Contour plots of suspended matter concentrations over the measurement period and below 500mg/L. Numbers along x-axis is day number since 01/jan/2011. Numbers along y axis denote height above the seafloor in cm.

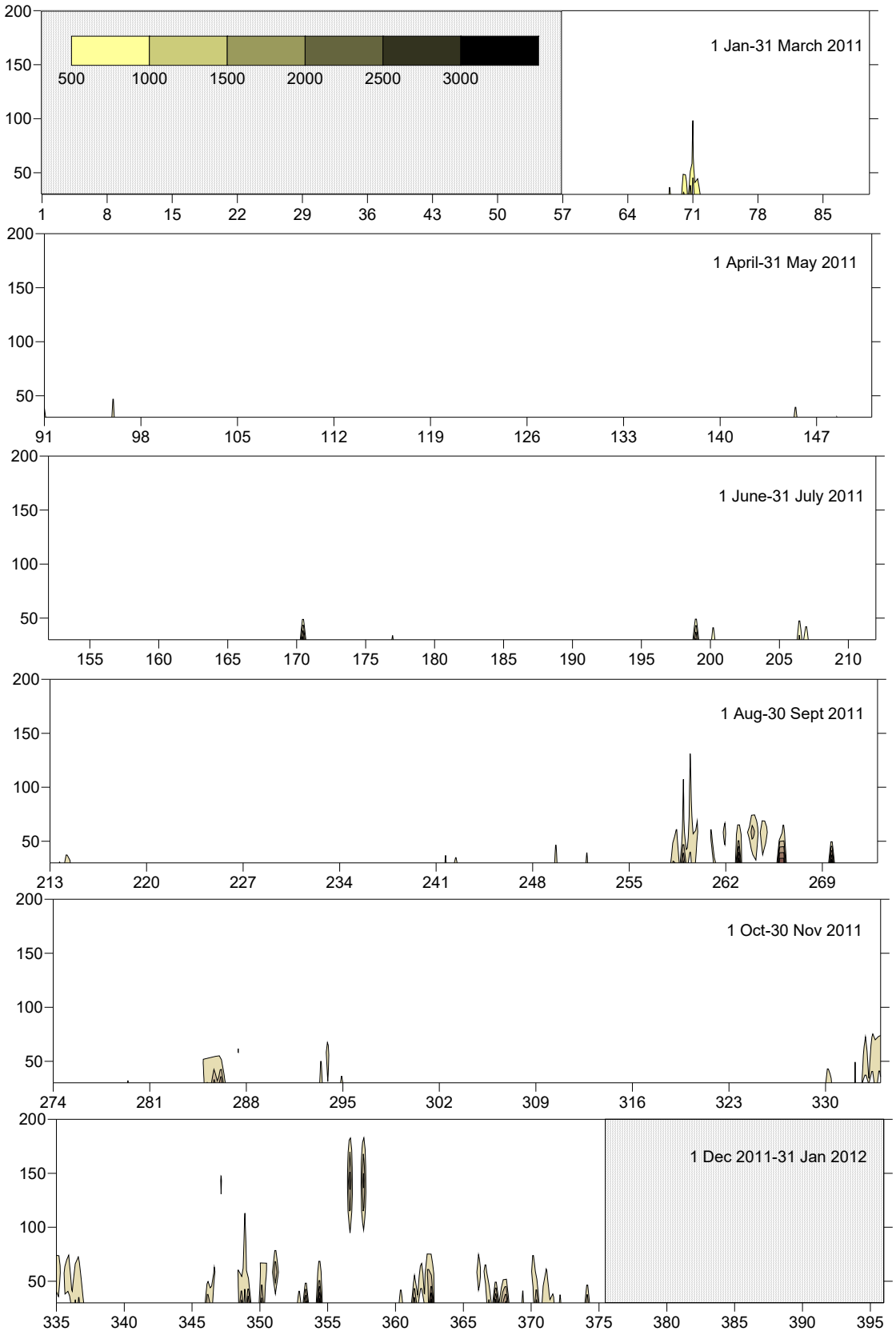

Figure 24. Contour plots of suspended matter concentrations over the measurement period and exceeding 500mg/L. Numbers along x-axis is day number since 01/jan/2011. Numbers along y axis denote height above the seafloor in cm.

Suspended matter.

Fluorescence and turbidity has been measured at four heights above the bottom. These data have been summarized as contour plots (Fig 21-23) and in table 6. The maximum SPM concentration (3965 mg/l) was measured on January 5th, 2012 at 30 cm above the bottom during a severe storm. At that time current velocities peaked at about 1.0 m/s. Peak measurements with values surpassing 2500 mg/L mainly occurred in the period September-December 2011 and in the beginning of 2012. This is best illustrated in Figure 23 in which a contour plot of only those SPM concentrations surpassing 500 mg/L is given.
Maximum Chlorophyll-a concentrations were measured in April and May during the spring phytoplankton bloom (Figure 21-Figure 25). Highest chlorophyll and suspended matter concentrations were always measured closest to the seafloor (Figure 24).

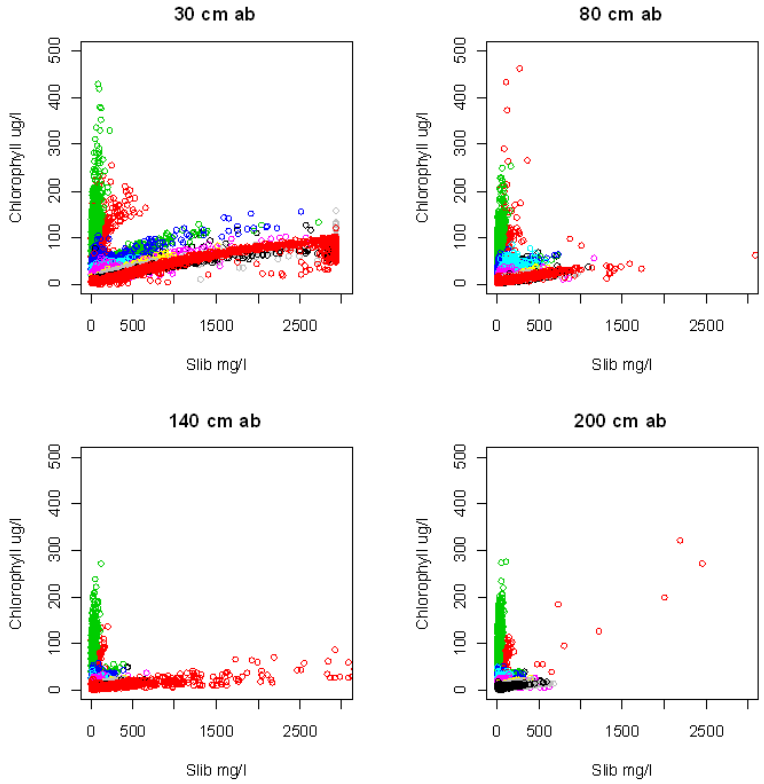

Figure 25. Seasonal change in the ratio between chlorophyll and SPM at the four heights above the seafloor at which these parameters have been measured. The four panels show a decrease of the absolute concentrations SPM. Highest absolute concentrations are measured at 30 cm ab. At greater heights above the seafloor concentrations decrease. Ratios at 140 and 200 cm are almost similar. Over time (colors=months) the changing ratio is illustrated by the changing slopes of the dots.

The seasonal development of the phytoplankton with a spring bloom causes that the qualitative characteristics of the material highly differs between seasons. This is depicted in Figure 26. In this figure the Chlorophyll concentrations have been plotted against turbidity. During the spring bloom (April – May) the ratio between both dramatically increases, visualized as increasing slopes, ultimately resulting in two clusters of material in May. After May this separation gradually disappears.

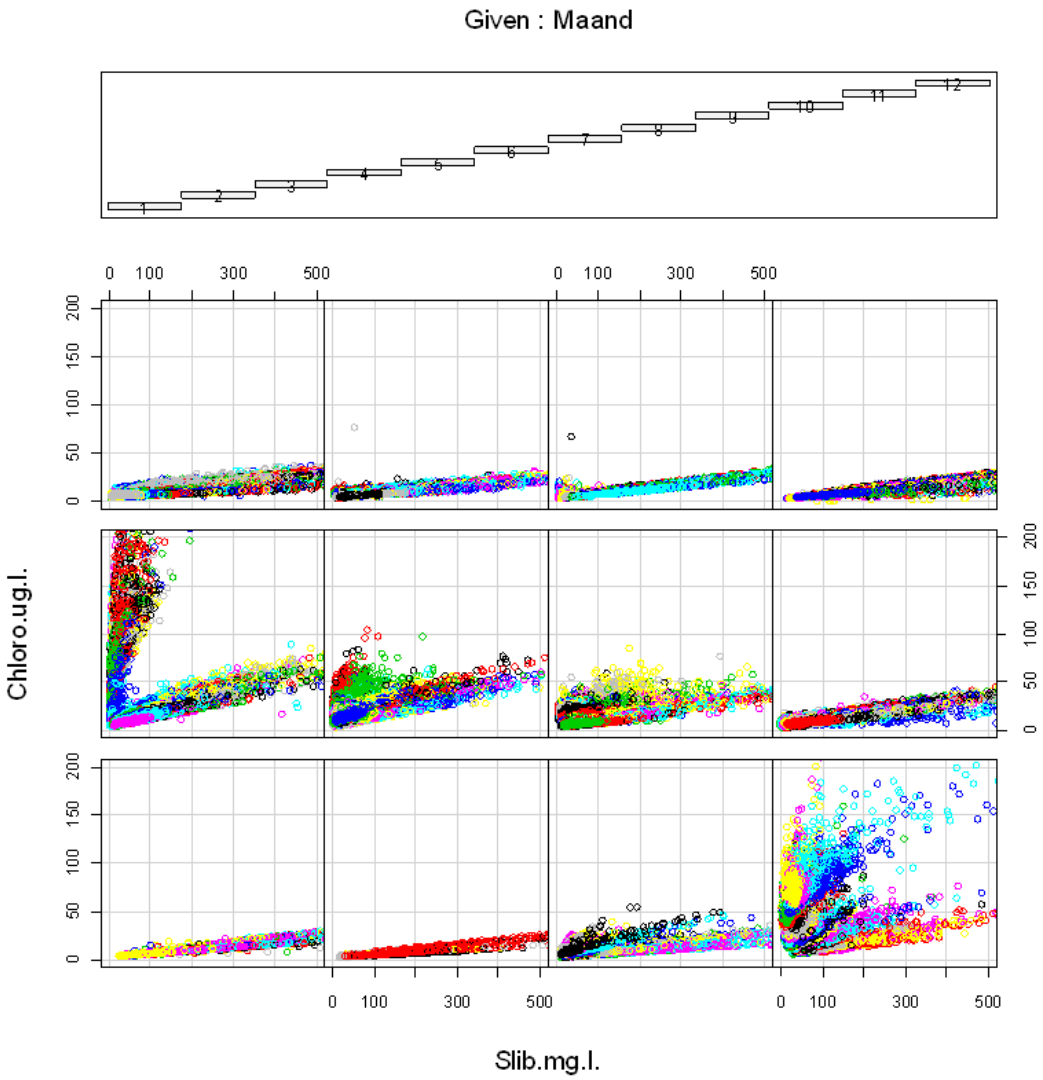

Figure 26. Seasonal change in the ratio between chlorophyll and SPM. Lowest row is January to April, Middle row is May to July and top row denotes the month September to December. Similar symbol colors within each panel indicates values measured at the same day. It is clear that in April there is a gradual change from a low ratio SPM material to a double peaked spectrum in May. In the months following the spring bloom the spectrum becomes narrower suggesting that the chlorophyll rich part of the SPM gradually disappears.

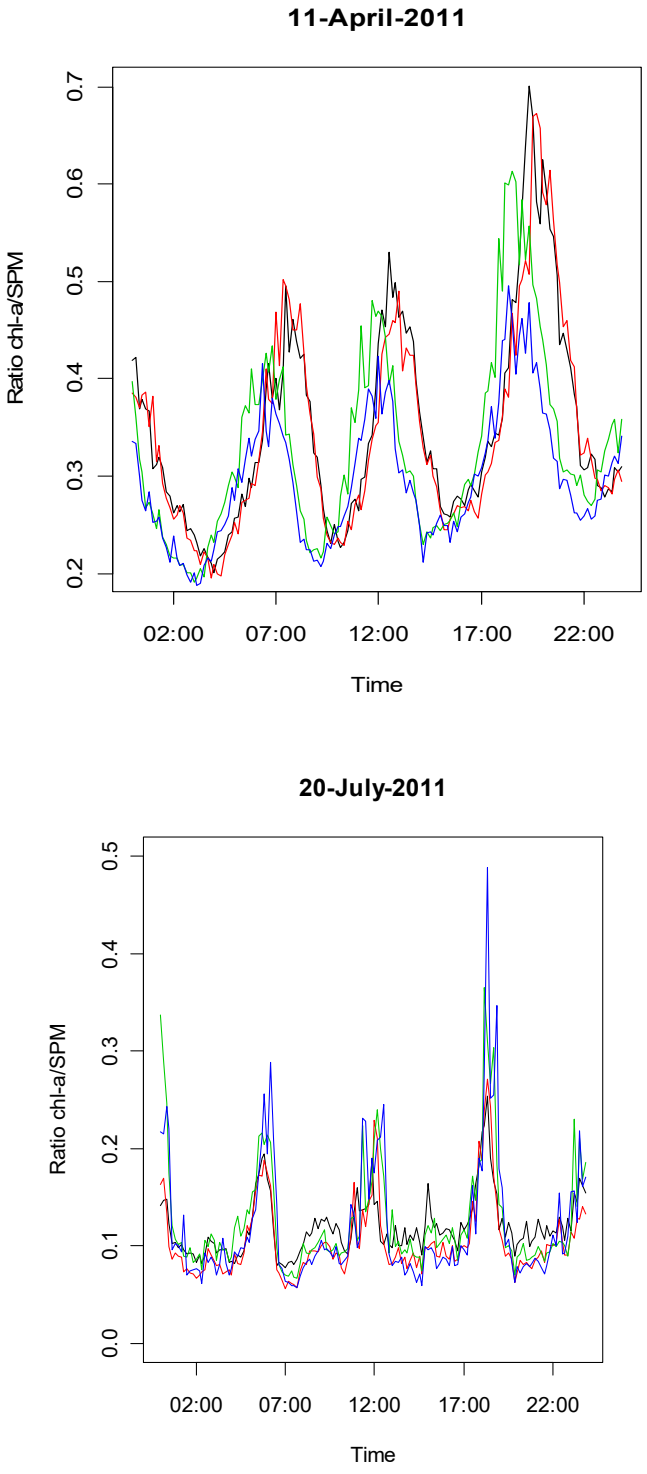

Figure 27. Tidal change in the ratio between chlorophyll and SPM. Black line 30cm above the bottom, redline, 80cm above bottom, blue line 140cm above bottom and green line 200 cm above bottom. Note for 11 April 2011 the time lag at which the peakvalues are measured between the two highest and two lowest height levels.

There is also a marked tidal cycle and seasonal variation in the ratio of SPM and Chlorophyll (Figure 27). This cyclic suggests that the chlorophyll rich particles and the inorganic SPM are partially coupled This is most obvious when expressed as the ratio of chlorophyll to turbidity and plotted against time. This shows that tidal phenomena steer the quality of the material. Such tidal effects are evident in all seasons but most obvious in spring when the amounts of fresh chlorophyll is highest due to the spring bloom. The data suggest that the suspended material

behaves like a blanket of material above the bottom. When a “blanket” of SPM settles during slack tide, it first passes the highest sensors followed by passing the two bottom ones, i.e. 80 and 30cm. Especially the time difference between the top two and bottom two sensors is evident and is most likely related to the sequential settling of material with different densities in combination with the height difference between the four sensors. Later in the year the time difference of settling material passing the each of the four sensors, becomes less obvious. This is thought to be related to the absence of two types of SPM present as being illustrated in Figure 26 and 27.

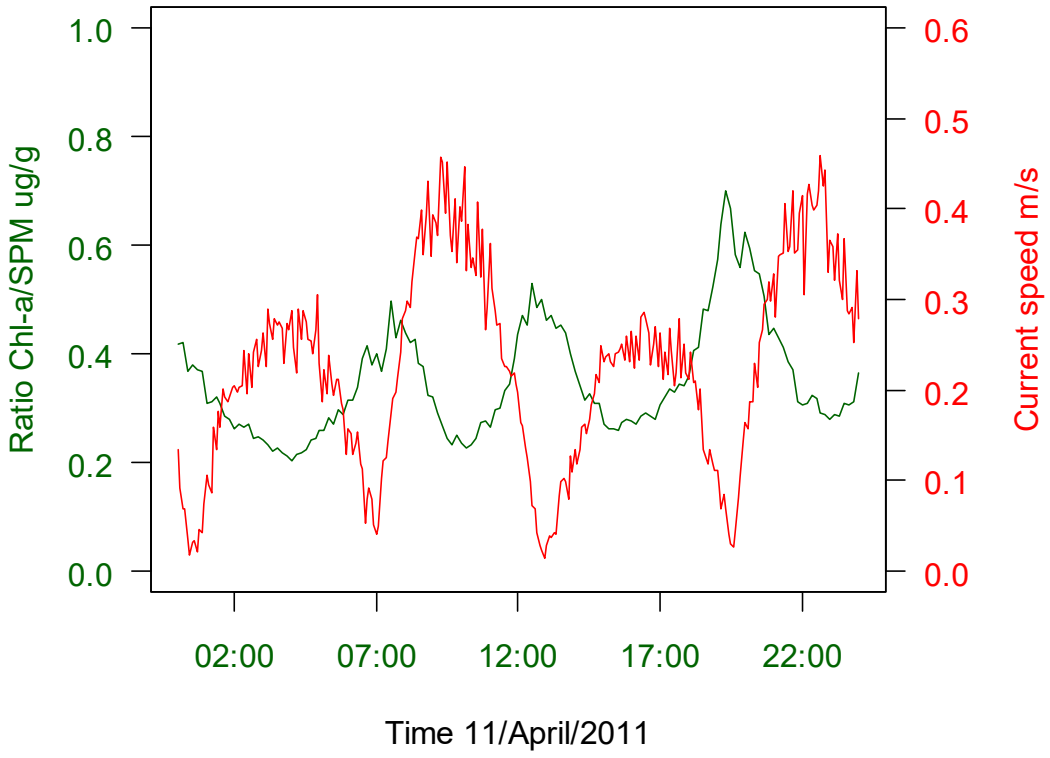

Figure 28. The ratio between chlorophyll and SPM at 30cm above the bottom (greenline) together with the current speed at 140 cm above the bottom (redline). There is a marked tidal variation in the ratio suggesting that high ratio material has a lower settling velocity and that at or shortly after slack tide comes into reach of the seafloor.

The observed chlorophyll / SPM Ratios are highly dependent on near bottom current speeds (Figure 28). At increasing speeds gradually heavier (chlorophyll-mud-sand) particles become resuspended, hence cause a changing ratio and thus a change in the quality of the food available for filter feeders. The effects of current speed on the quality of the resuspended material is especially evident in the months (April-May) when freshly produced organic phytodetrital material is present (Figure 29).

The effects of different resuspension and settling characteristics is especially evident during periods with quiet weather when wind induced wave and current effects are minimal.

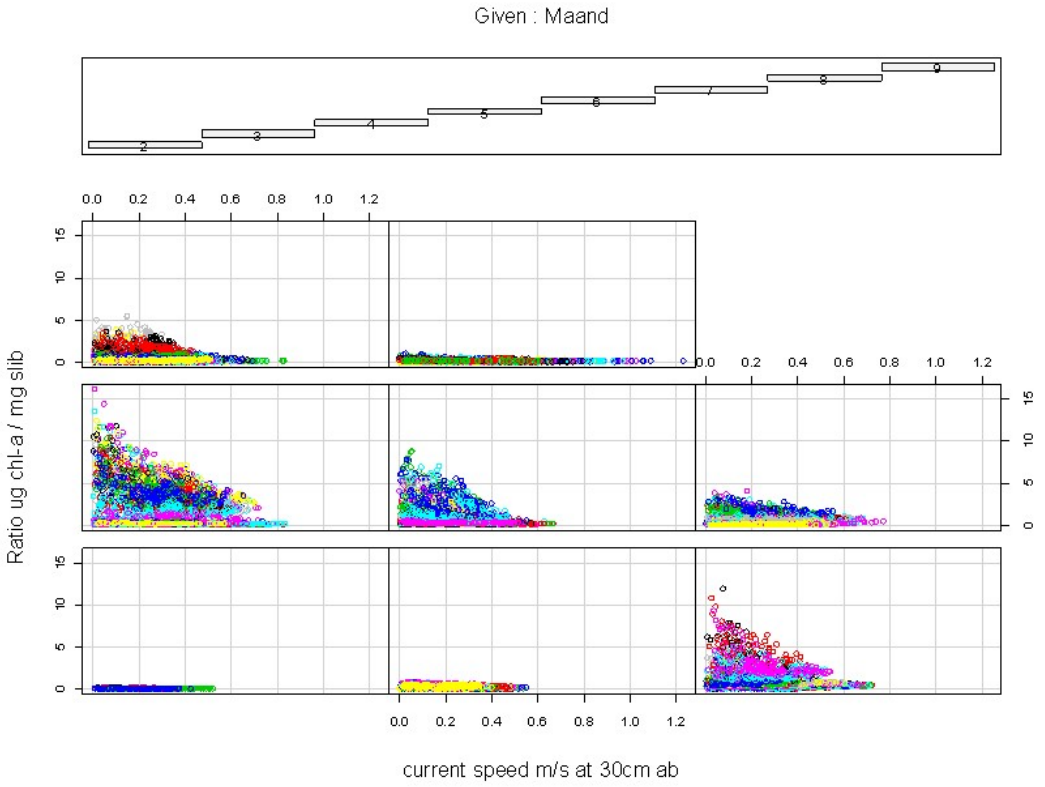

Figure 29. Seasonal change in the ratio between chlorophyll and SPM at 30cm above the seafloor. Lowest row represent February to April, Middle row represents May to July and top row denotes the month August and September. Similar symbol colours per panel indicates values measured at the same day. In the months that freshly produced organic material is available (April-August) the ratio of the suspended material decreases with increasing current speeds implying that there is a marked difference over the tidal cycle in terms of quality of the material which can be utilized as food for filter feeders.

The limited water depth at the deployment location makes the bottom “vulnerable” to effects of waves. This is best illustrated when the record of suspended matter and wave heights are superimposed on each other (Figure 30). Over the entire year increased concentrations of suspended matter are found during or shortly after wave events. Qualitative comparison with wind records (KNMI) suggest that these wave events are all related to storms. The effects are especially evident during the autumn-winter storms at the end of 2011 and in the beginning of 2012. The resuspension of material not only caused an increase in the concentration of suspended matter, but concentrations of chlorophyll also increased significantly. This suggests that fine particles with attached chlorophyll are released from the sediments and that this fraction potentially acts as a “food bank”. The exact origin of this material is unclear. It might represent freshly buried pelagic phytoplankton which is sequestered in the bottom before it is released by a storm event. Alternatively it can also point to a local source in the form of epi-phytobenthos brought into the water column during severe wind events. Especially the shallower fore shore parts (less then 10 meter) might host such a epi-phyto-benthic community. In this zone, light penetration is potentially high enough to promote primary production at the seafloor. Subsequent export of this material might likewise explain the high concentrations of chlorophyll in the bottom layer during and shortly after storms. It might also contain the clue why densities of *Ensis directus* are highest, close to the coast (BWN 2011, unpublished results).
During the lander servicing on June 24th two ships were working on beach nourishments close to the lander. The effects of these ship operations might be visible as slightly increased SPM concentrations in the period around day 173 (Figure 22,23). The range of SPM concentrations at

30 cm above the bottom during that day was between 54 and 729 mg/L. These values fit within the SPM concentration ranges as reported in table 6 for other periods of the year.
Figure 31 gives a frequency distribution for the Log(SPM) concentrations for June 24th, the entire month of June and the entire year. This figure suggest that on June 24th during beach nourishments, high SPM concentrations occur slightly more frequent when compared to the monthly average or the entire year (without the month of June).
However the absolute SPM concentrations during that day are far below peak concentrations caused by resuspension by wind and wave events (Figure 30) later during the year.

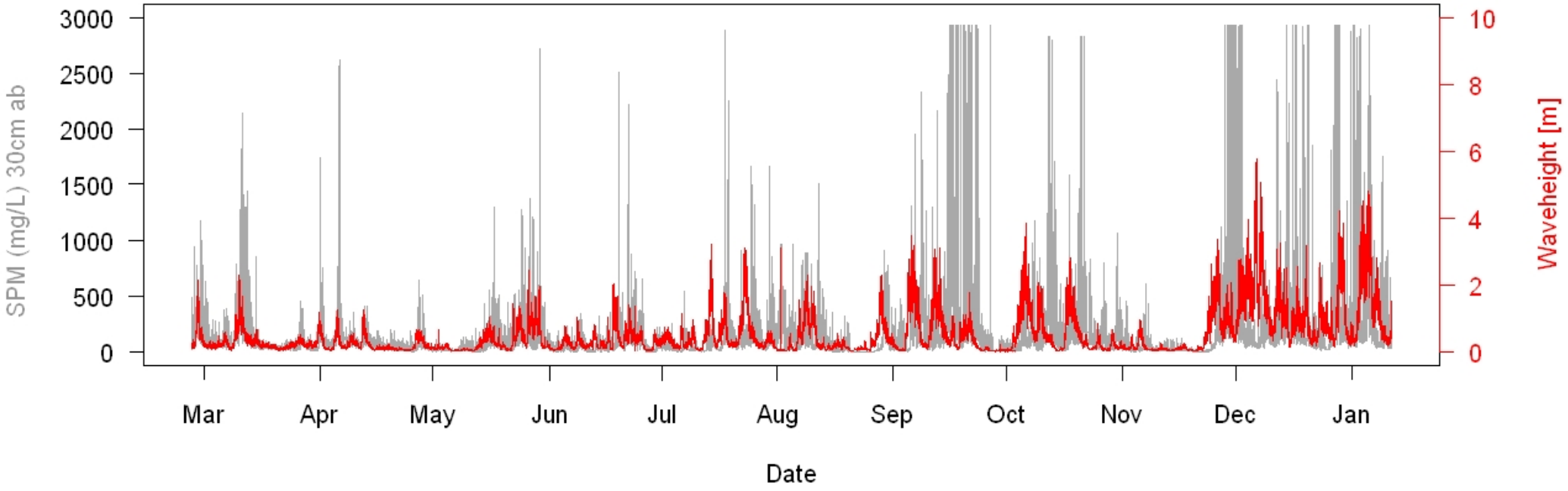

Figure 30. Temporal alignment of the SPM concentration and the wave heights measured at 10 minute intervals. The alignment of “wave events” and increases in the concentration of suspended material at a height of 30 cm above the bottom is evident. Concentrations of suspended material tend to lag a little behind the increased wave heights. This suggests that time is needed to free material from the sediment and / or that the (some) peaks in SPM refer to material which originates from locations away from the point where measurements were being made.

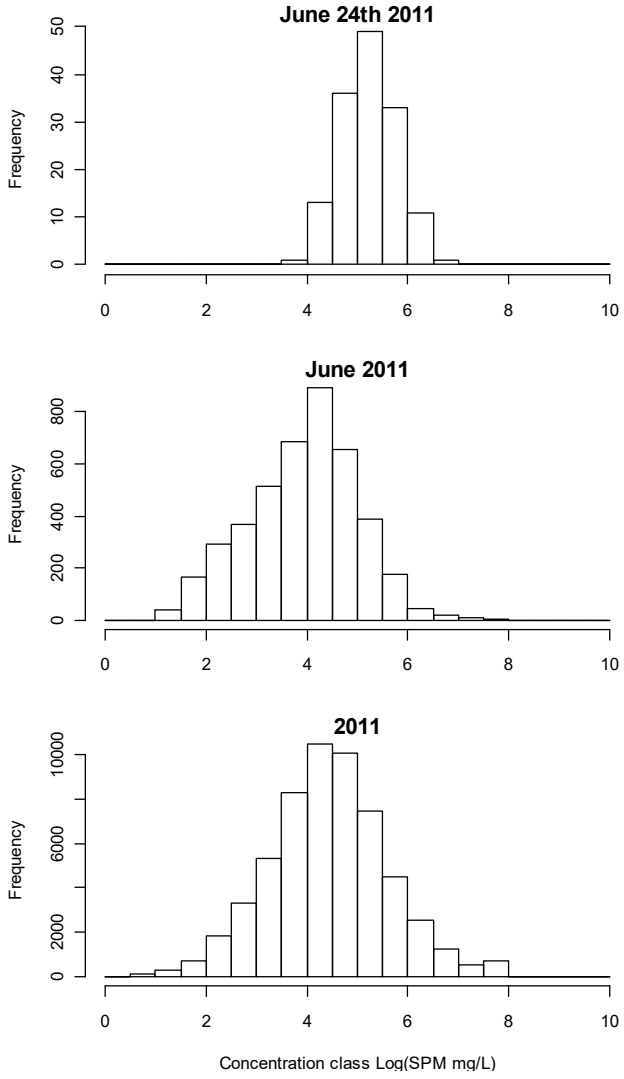

Figure 31. Comparison of the frequency of occurrence of SPM concentrations. SPM in Log (concentration). Measurement frequency was 1 measurement/10 minutes.

Table 6. Overview of monthly average ± SD, minimum and maximum concentrations of SPM and Chlorophyll measured at four heights above the seafloor at ~ 10 meter water depth off the coast of Egmond.

Month	Month nr	Height above bottom (cm)	AVG SPM [mg/L]	SD SPM	Max SPM [mg/L]	Min SPM [mg/L]	AVG Chloro [ug/L]	SD Chloro	Max Chloro [ugr/L]	Min Chloro [ugr/L]
Feb-11	2	200	116.6	65.7	414.4	17.4	5.2	1.9	12.9	2.4
Mar-11	3	200	59.8	47.6	519	7.2	5.8	2.8	22.5	2.5
Apr-11	4	200	63.9	70.9	2452.4	11.6	30.5	22.9	322.3	5.5
May-11	5	200	46.3	39.6	418.8	2.5	42.3	40.3	276.4	4.5
Jun-11	6	200	38.1	34.5	314.6	1.9	16.9	6.9	52.6	3.3
Jul-11	7	200	48.7	38	460.7	3.7	12.7	6.7	42.6	3.2
Aug-11	8	200	52.4	53	630.2	0.9	8	2.7	27.1	2.9
Sep-11	9	200	90.4	73.3	674.6	6.5	7	2.3	22.8	3.2
Oct-11	10	200	71.6	53.2	597.8	4.4	5.9	1.7	19.8	2.9
Nov-11	11	200	-	-	-	-	-	-	-	-
Dec-11	12	200	-	-	-	-	-	-	-	-
Jan-12	1	200	-	-	-	-	-	-	-	-
Feb-11	2	140	137.6	80.6	506.1	18.5	5.9	2.1	14.2	2.7
Mar-11	3	140	67.2	59.2	617.2	6.7	6.6	3.4	28.7	2.7
Apr-11	4	140	58.9	39.1	441.3	3.9	30.2	21.1	142	6.8
May-11	5	140	53.9	48.2	385.7	2.3	42.2	37.4	271.6	4.9
Jun-11	6	140	43.4	37.6	385.7	1.9	18	7.5	58.8	3.7
Jul-11	7	140	51.7	41.4	664.7	3.7	12.9	5.8	44.7	3.5
Aug-11	8	140	50	51.9	398.9	0.9	8.2	3.1	28.3	3
Sep-11	9	140	92.1	75.4	754	6.7	7.9	2.8	25.9	3.6
Oct-11	10	140	84.4	62	657	4.9	6.5	2.1	22.9	3
Nov-11	11	140	53.4	88	2917	3.7	5.1	3.3	87.2	2.4
Dec-11	12	140	181.4	382.8	3661.3	18.1	7	6.5	130.8	2.6
Jan-12	1	140	134	95.6	1294.1	27.3	6.7	2.7	21.6	3.1
Feb-11	2	80	161.9	99.7	669.1	21.5	5.7	2.4	16.9	2.3
Mar-11	3	80	78	79.8	867	6.9	5.8	3.3	30	2.3
Apr-11	4	80	71.8	57.6	1012.2	4.6	35.8	29.7	461.6	5.3
May-11	5	80	71.7	71.3	720.9	3	41.7	37.3	253.3	3.9
Jun-11	6	80	59.2	57.5	735	2.5	19.9	9.2	74.6	4.3
Jul-11	7	80	81.2	70.9	1162.6	4.9	15.1	9	85.3	4.1
Aug-11	8	80	68.9	76	615.6	1.2	8.7	4.1	36.9	2.7
Sep-11	9	80	115.3	99.6	961.5	7.6	8.6	3.3	31.5	3.7
Oct-11	10	80	119.3	102.1	1093.9	5.6	7.4	3.5	37.4	2.6
Nov-11	11	80	62.5	90.5	960.5	3.5	5.7	3.8	36.6	2.6
Dec-11	12	80	137.3	121.7	1723.6	16.9	7.2	4	39.1	2.6
Jan-12	1	80	177.7	188.4	3964.8	30.1	8.5	4.9	81.5	3.4
Feb-11	2	30	247.3	175.8	1187.9	29.6	12.4	7.1	45.3	3.6
Mar-11	3	30	117.2	162.6	2150.7	8.4	10.8	8.3	81.8	3.6

Month	Month nr	Height above bottom (cm)	AVG SPM [mg/L]	SD SPM	Max SPM [mg/L]	Min SPM [mg/L]	AVG Chloro [ug/L]	SD Chloro	Max Chloro [ugr/L]	Min Chloro [ugr/L]
Apr-11	4	30	101.9	125.6	2626.7	5.8	42.3	30.1	254.3	9.7
May-11	5	30	112	148.8	2717.2	3.8	57.8	46.9	428.7	6.1
Jun-11	6	30	91.7	146.7	2507	2.6	27.3	14.2	155	5.5
Jul-11	7	30	115.4	173.5	2890.6	5.6	19.9	9.8	101.9	5.1
Aug-11	8	30	114.5	147.1	1519.3	1.3	13.4	8.2	82.5	3.8
Sep-11	9	30	308.8	540.6	2925.9	7.6	18	16.7	157.6	4.2
Oct-11	10	30	217.1	301.5	2833.1	7.1	12.8	9.6	84	3.6
Nov-11	11	30	143.3	396.4	2925.9	4.1	9.3	12.5	101.9	2.9
Dec-11	12	30	332.9	567.5	2925.9	18.9	15.6	18.5	102	0.2
Jan-12	1	30	378.3	507	2925.9	30.7	18.6	18.5	120.5	4
Average	1-12	200	**65**	53	720	6	**15**	10	89	3
Average	1-12	140	**84**	88	1057	8	**13**	8	73	4
Average	1-12	80	**100**	93	1207	9	**14**	10	99	3
Average	1-12	30	**190**	283	2511	10	**22**	17	143	4
Average		30-200	**113**	134	1418	9	**16**	11	102	4

Valvometry

The mussels (*Mytilus edulis*) used in the valvometry experiment had a high survival rate. Up to September 2011 only three mussels died. A leaking connection in two of the sensor plugs prevented collection of reliable data from two channels in spring and later in autumn winter the same happened. Massive barnacle overgrowth during the summer limited in some periods the maximum valve gape of the mussels, i.e. the amplitude decreased. In the analyses a trend correction has been applied to correct for this.

With 50-60 %, mortality of the *Ensis* used in the *in-situ* valvometry, was high. Especially in summer the mortality increased due to predation by crabs. Despite the high mortality a fair number of good records of *Ensis* valve movements were collected. A selection has been made of only those sections of the valve movement records which were of sufficient length.

For both mussels and *Ensis* the raw data were transformed to a relative valve opening (fraction from 100% open) and related to environmental data which were collected at the same time.

MUSSELS

In figure 32 records of 5 mussels for the second deployment period is given. On average the valve gape of the mussels is between 75 and 81 % of the maximum value measured. Over time a cyclic pattern is visible. A pairplot of all datapoints (Figure 33) only shows a weak positive correlation although in all combinations the maximum openings fractions are positively

correlated to each other. Closer inspection shows that this is an effect of a temporal change of the correlation over time between any of the combinations of individual valve gape signals (Figure 34). A Pairplot (Figure 35) of the running correlations illustrates that all temporal correlations yield positive a trend. suggesting that there is a common trend in the timing of valve gape behaviour. This suggests a temporal change in environmental forcing on the valve gape of mussels.

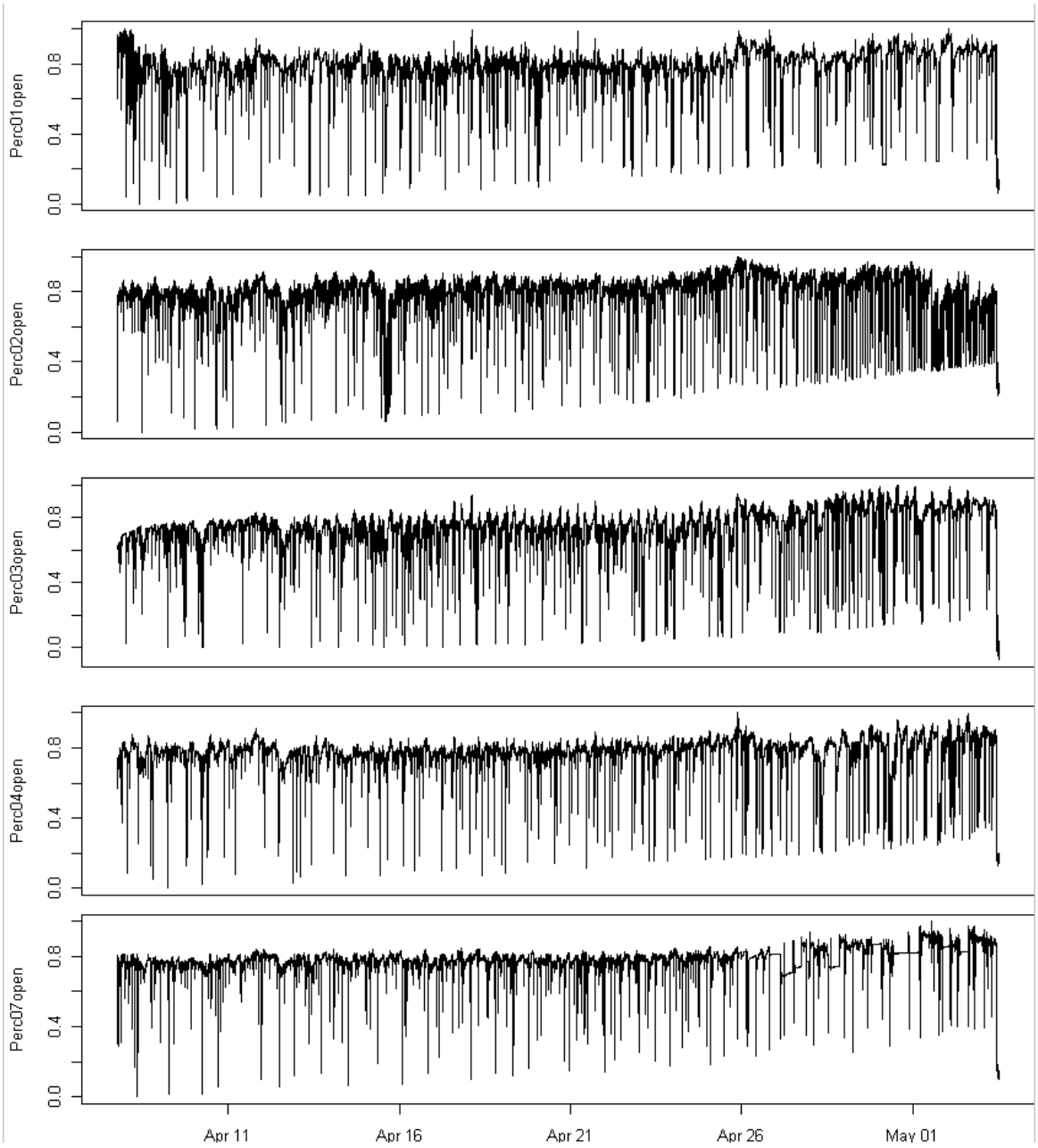

Figure 32. Example of the valve gape record of 5 mussels in the second deployment period of 2011.

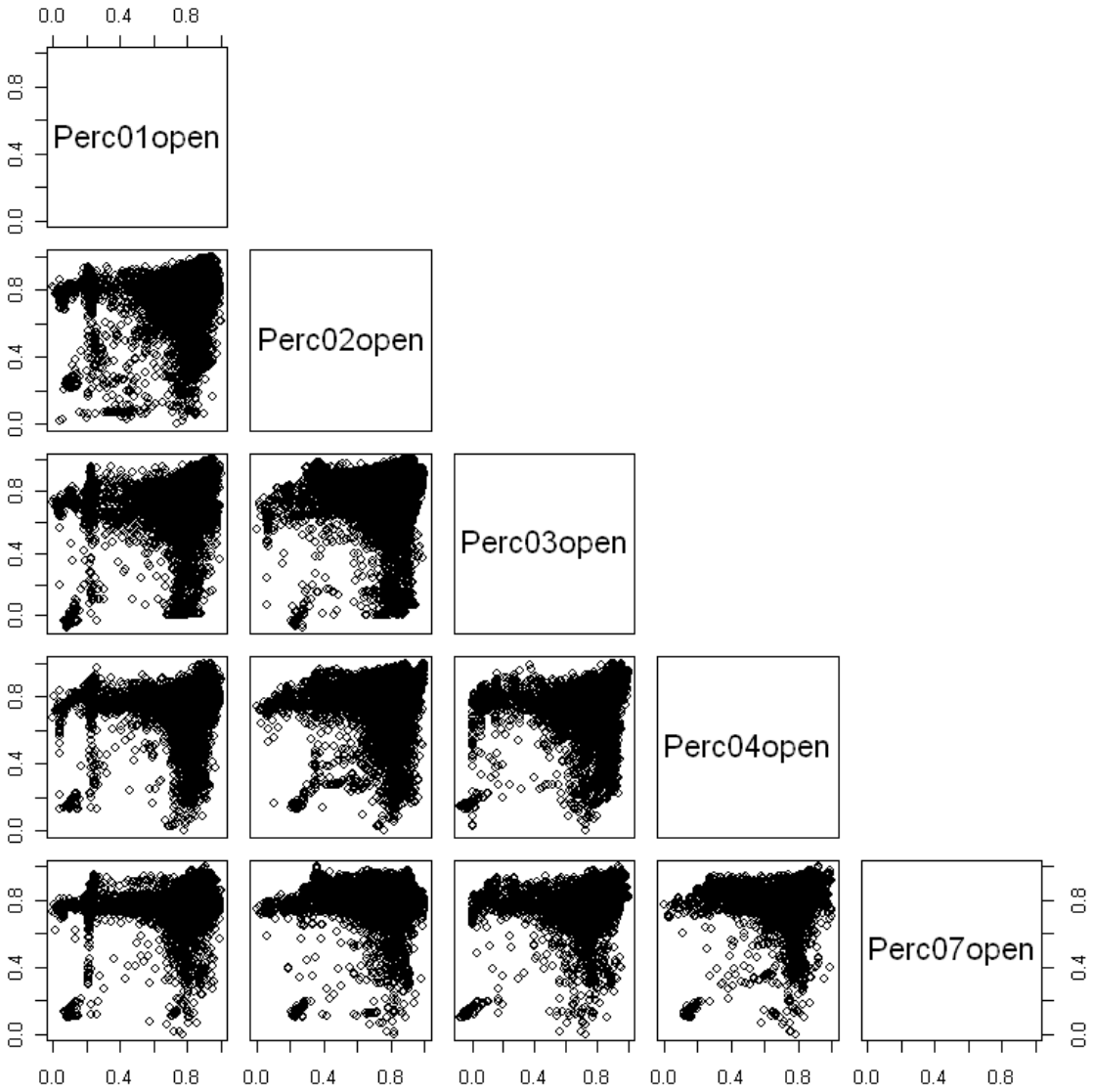

Figure 33. This pair plot gives the relationship of the valve opening signals of the same set of mussels as given in figure 26. The maximum valve opening of the mussels is strongly related but the clarity of the signal is partly obscured by the number of uncorrelated valve movements.

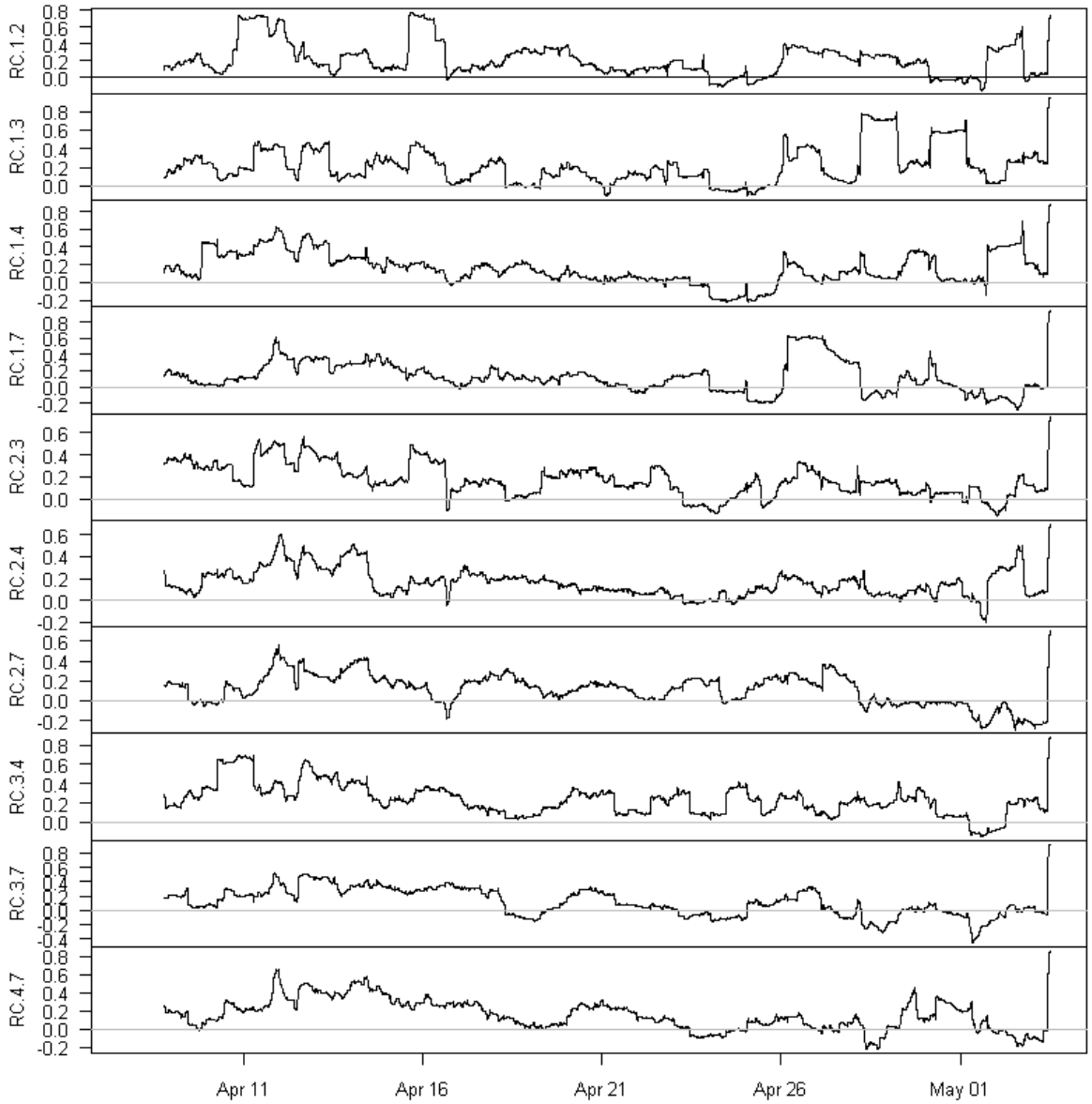

Figure 34. A plot comparing the running correlation between any of the combinations of two animals given in figure 26. The line gives the height of a running correlation over a time frame of 1440 minutes (1 day). For many combinations the correlations have a temporal alignment. Coding of the y-axes; RC=Running Correlation and numbers indicated depicted combination of animals compared, i.e. 1.2 means the running correlation of animal 1 and 2 etc.

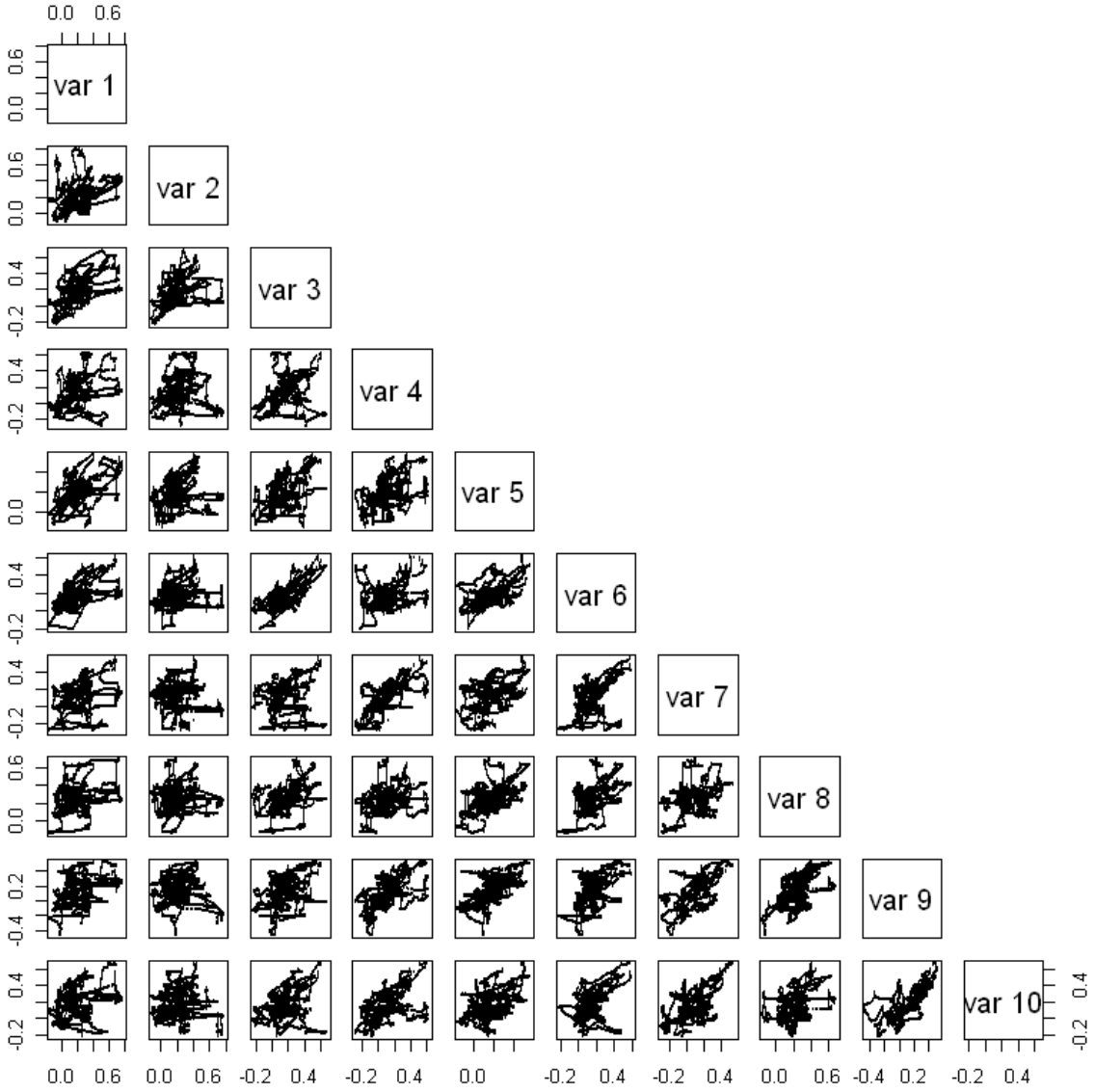

Figure 35. A pairplot illustrating the temporal alignment of the running correlations for all possible combinations as given in figure 34. All combinations yield positive trends i.e. the poorly correlated and highly correlated periods among all animals have a similar timing. This suggests a temporal change in environmental forcing on the valve gape of mussels.

ENSIS

Survival of *Ensis* in the in-situ set up is much lower than that of mussels. This partly because predation but certainly also has to do with the sensitivity of this species as has been observed in other studies. Nevertheless we have been able to collect every deployment period several time series of valve gape of animals which survived most of or the entire deployment period. The records collected between week 14 and 18 and between week 18 and 22 have been analysed in more detail.

The records show a great resemblance to those collected from mussels although the frequency of occurence of absolute valve closures seems to be less. After each closure incidence the *Ensis* needs a longer time to recover and reach its maximum valve gape again.

An example of valve gape records for *Ensis* given in figure 36 (wk14-wk18) and in week 31 (wk18-wk22). Figure 37 also illustrates records of animals which died either soon after deployment or at the end of the deployment period.

The similarity of the *Ensis* valve gape signals obtained in these two different periods and among the different animals is compared in figure 38 and figure 39. The difference in similarity between the two sets of time series is extremely clear from the comparison of these pairplots. The pairplot for period wk18-22 (fig 39) illustrates that the *Ensis* in that period had better synchronised valve movements than in the preceding period (Fig 38). This is furthermore illustrated in figure 40 and figure 41 which shows the height of correlation between any combination of animals over a 1 day long time window. The figures both illustrate over which time intervals and for which animals the similarity between the two signals is high and thus shows that there is both variation in time and between animals.

If these time trends of signal similarity (correlations) is given as pairplots (figure 42 and 43) they demonstrate that the *Ensis* valve gape over time and between individuals has less synchrony than the signals obtained from mussels

In the next step of the analyses the valve gape has been compared to the measured turbidity at a height of 30 cm above the seafloor. Hereto the time series of valve gape and the timeseries of SPM concentrations were aligned on basis of time. The Turbidity record was split into classes on basis of concentration steps of 100 mg/l. For each *Ensis* the maximum valve gape within each of these classes was determined. The resulting condensed data series between valve gape and Turbidity were plotted against each other (Figure 44,Figure 45). These figures shows an inverse relationship between maximum valve gape and turbidity for all *Ensis*. Over the SPM concentrations measured (0~1500 mg/l) the approximate decrease in valve gape is about 20 %.

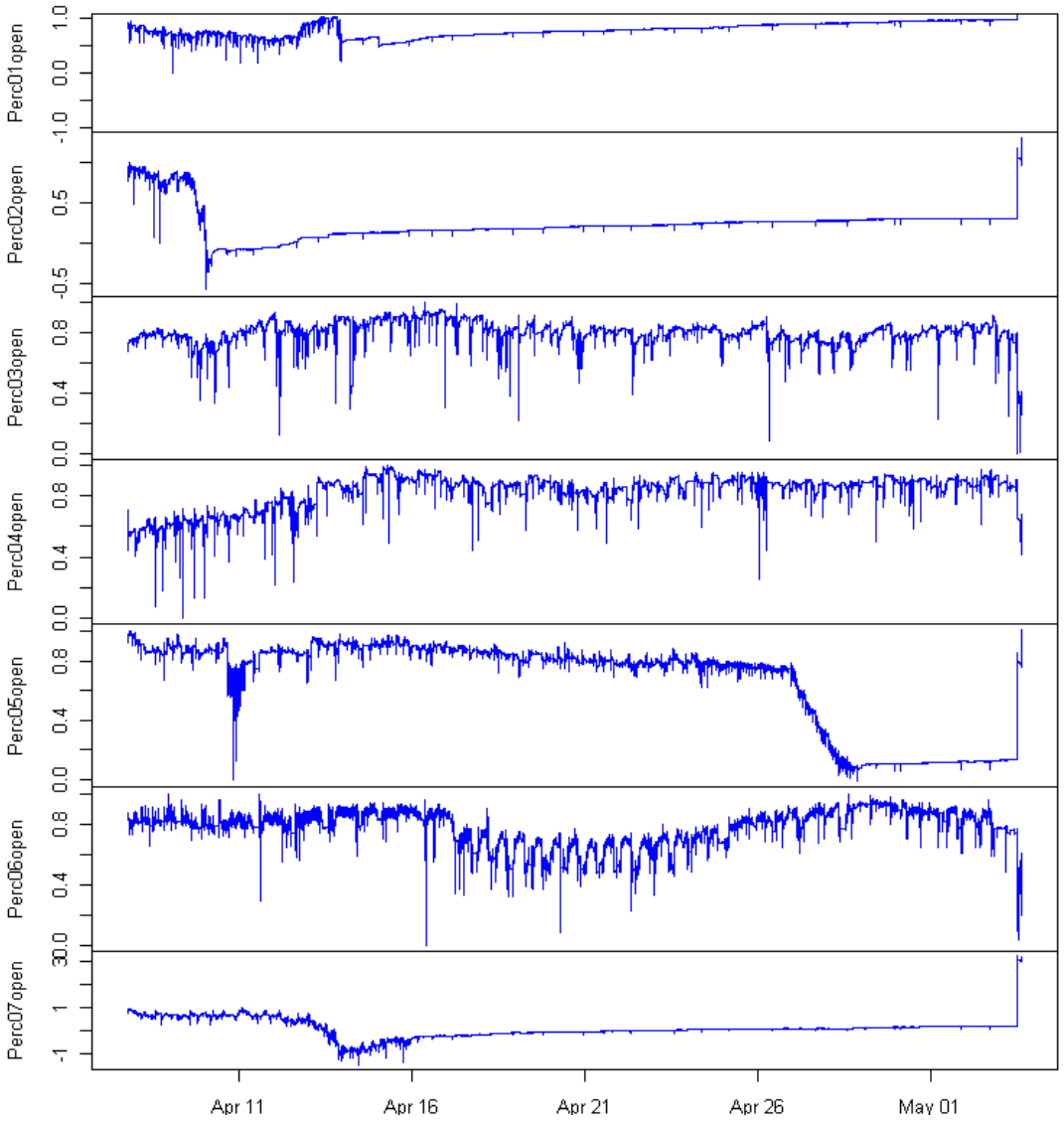

Figure 36. All valve gape records obtained from *Ensis directus* in the second deployment period (week 14-week 18 2011). Records 3 to 6 are believed to represent actual valve gape. Records 1,2 and 7 and the last part of record 5 illustrate the type of signal obtained from dying animals. These records are not taken in account in the further analyses.

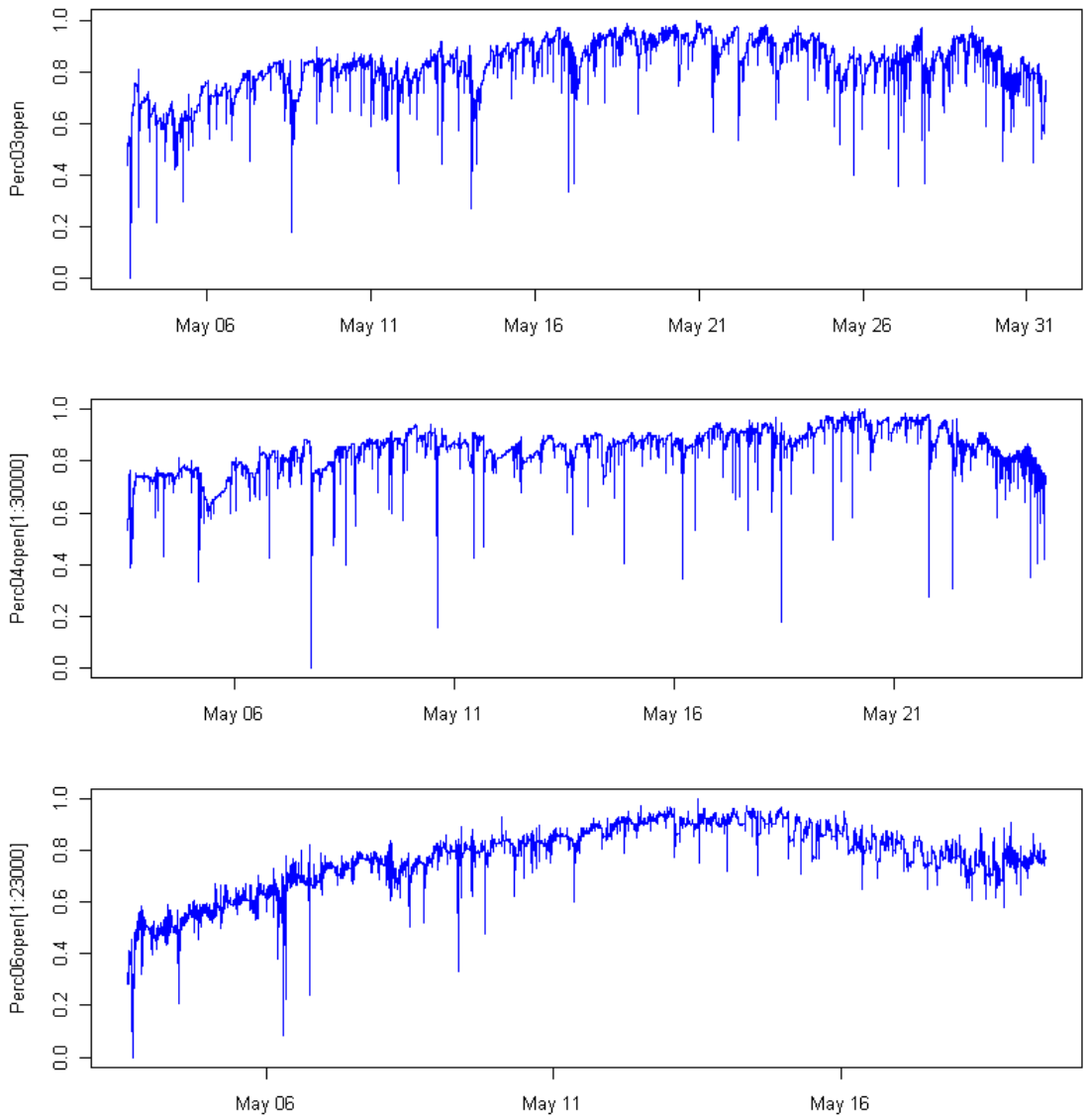

Figure 37. Valve gape records obtained from *Ensis directus* in the third deployment period (wk18 to wk22 2011).

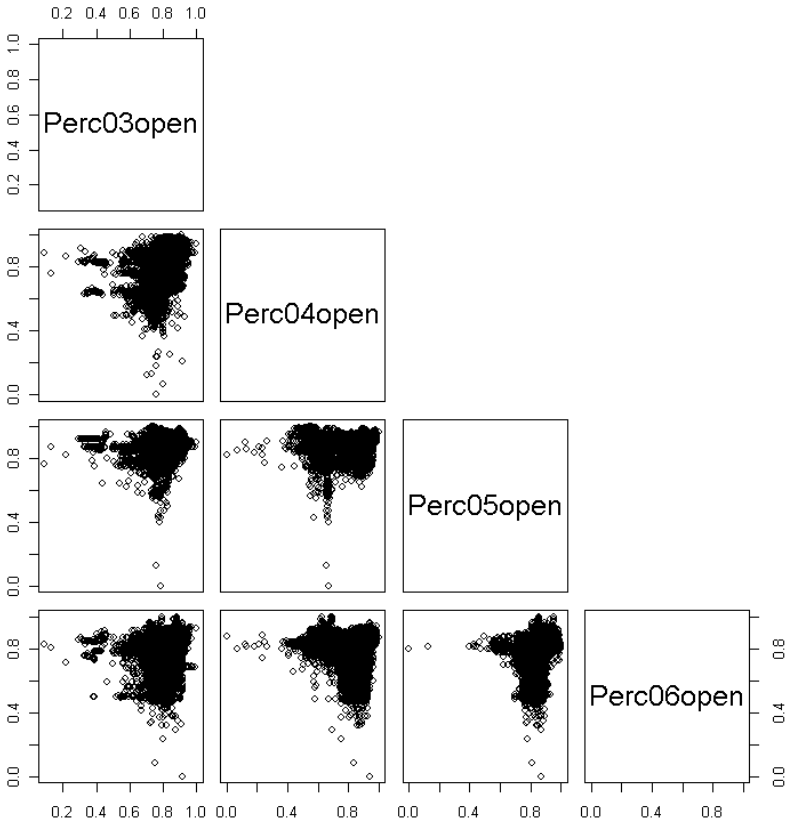

Figure 38. A pairs plot of the valve gape openings fraction of *Ensis directus* over measurement period wk 14 to wk 18 2011.

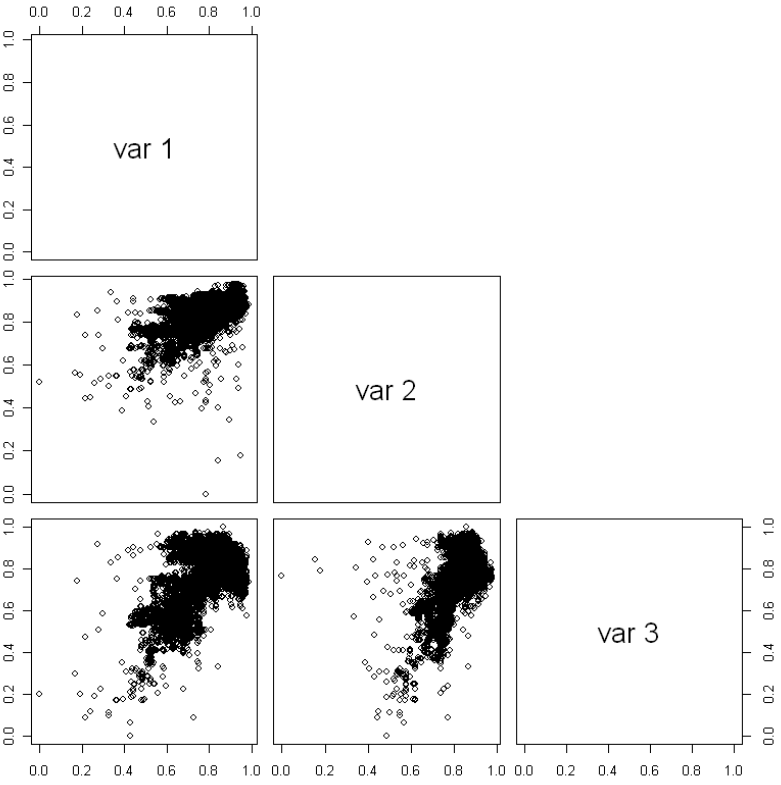

Figure 39. A pairs plot of the valve gape openings fraction of *Ensis directus* over measurement period wk 18 to wk 22 in 2011.

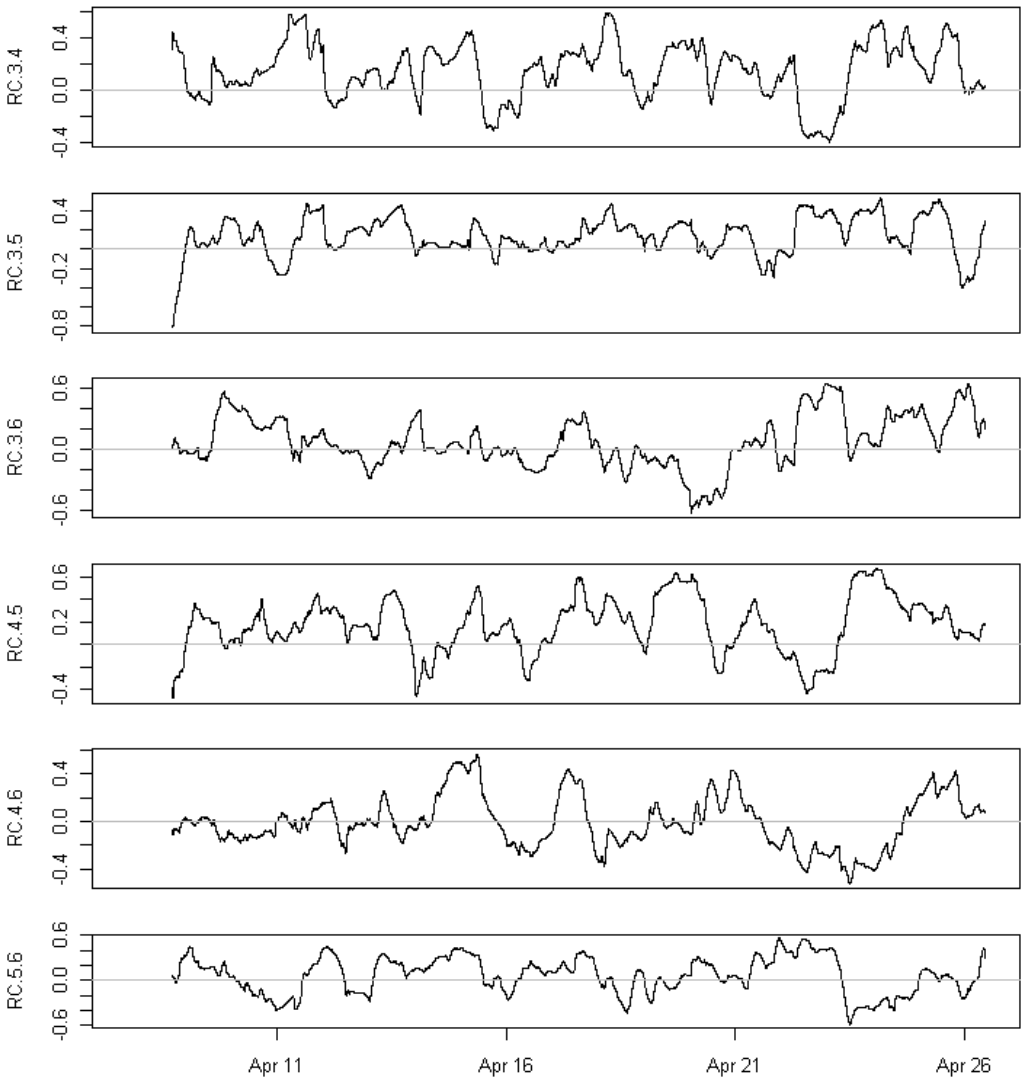

Figure 40. A plot comparing the running correlation between any of the combinations of two *Ensis*. The line gives the height of a running correlation over a time frame of 1440 minutes (1 day). For many time intervals and animal combinations the correlations have a good temporal alignment. Coding of the y-axes; RC=Running Correlation. Numbers indicate the tested combination of animals compared, i.e. 3.5 means the running correlation of animal 3 and 5 etc. Period; week 14-week 18 2011.

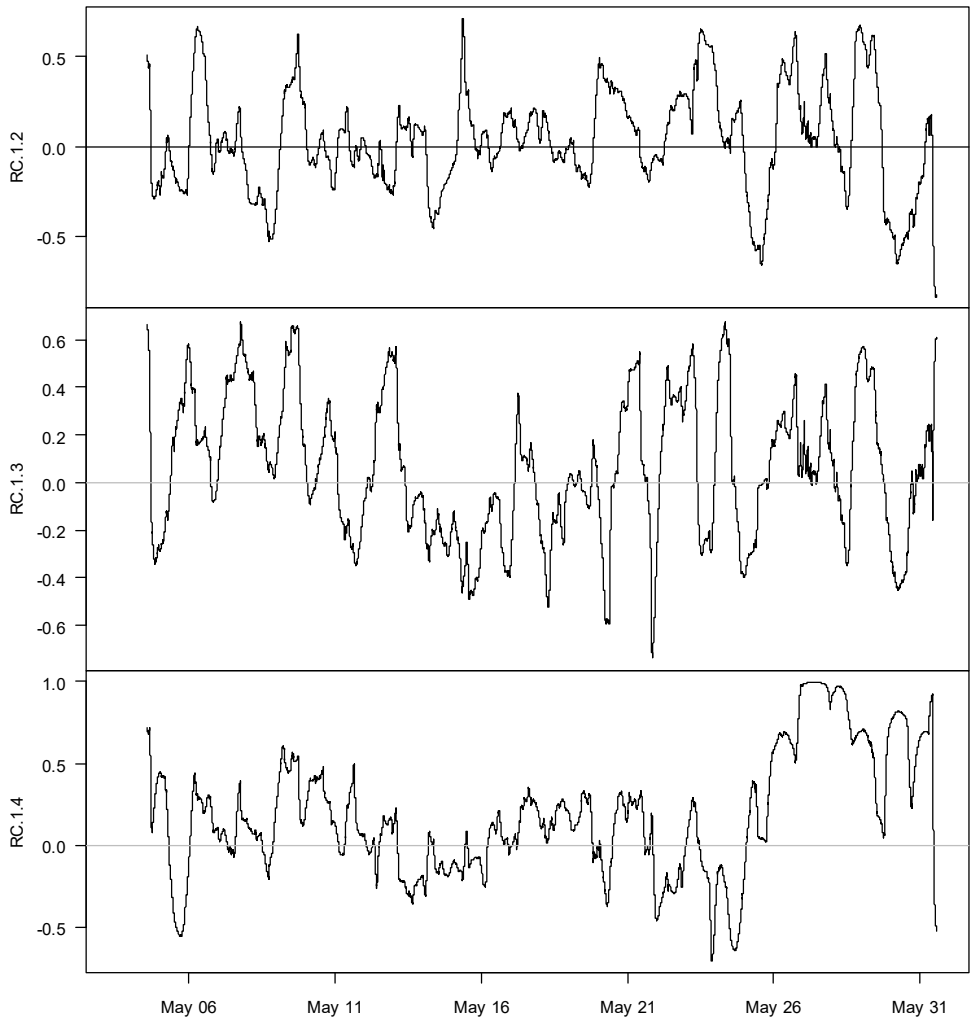

Figure 41. A plot comparing the running correlation between any of the combinations of two *Ensis* in the period between week 18 and 22. The line gives the height of a running correlation over a time frame of 1440 minutes (1 day). For many time intervals and animal combinations the correlations have a good temporal alignment. Coding of the y-axes; RC=Running Correlation. Numbers indicate the tested combination of animals compared, i.e. 1.2 means the running correlation of animal 1 and animal 2 etc.

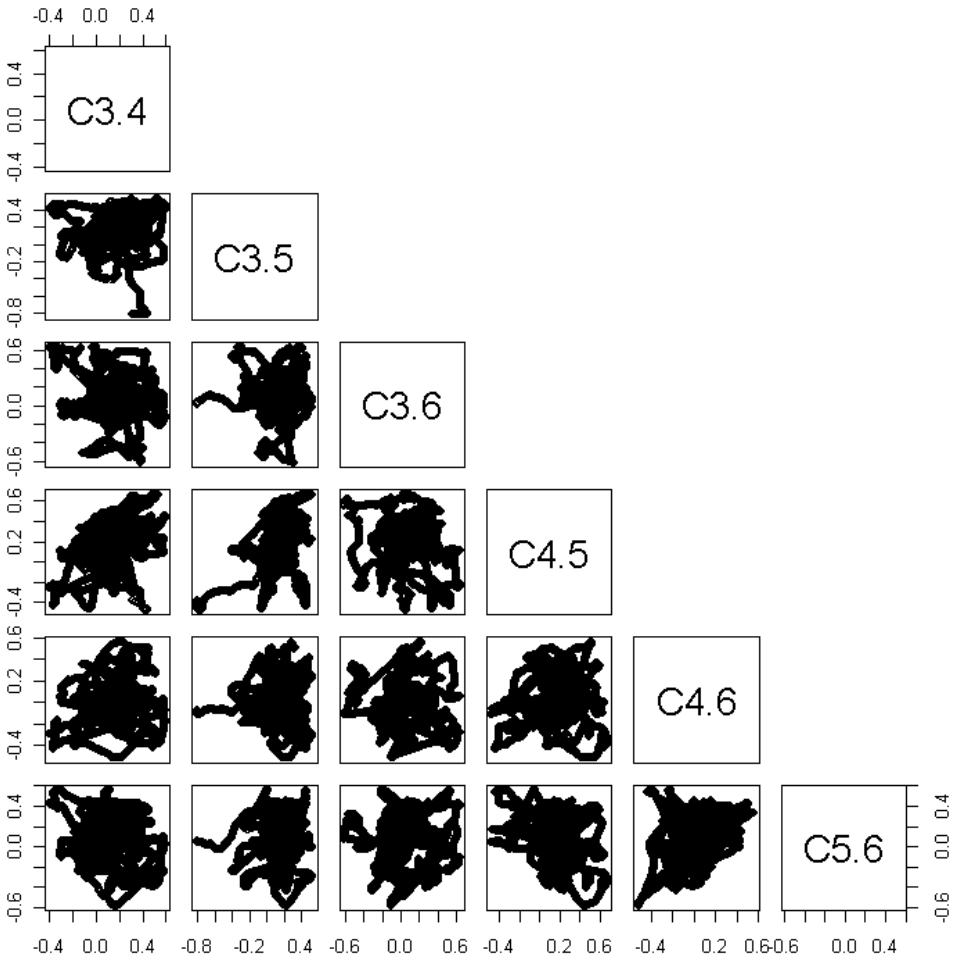

Figure 42. To check if all time series (wk 14_18) of correlations have well aligned similarities, the calculated running correlations were plotted as a pairplot to get an overview of the similarity of all possible combinations.

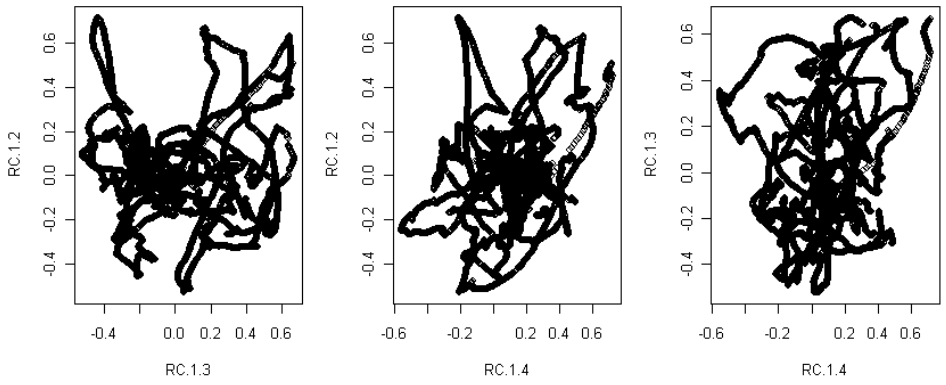

Figure 43. To check if all time series of correlations (wk 18_22) have well aligned similarities, the calculated running correlations were plotted as pair plot to get an overview of all possible combinations

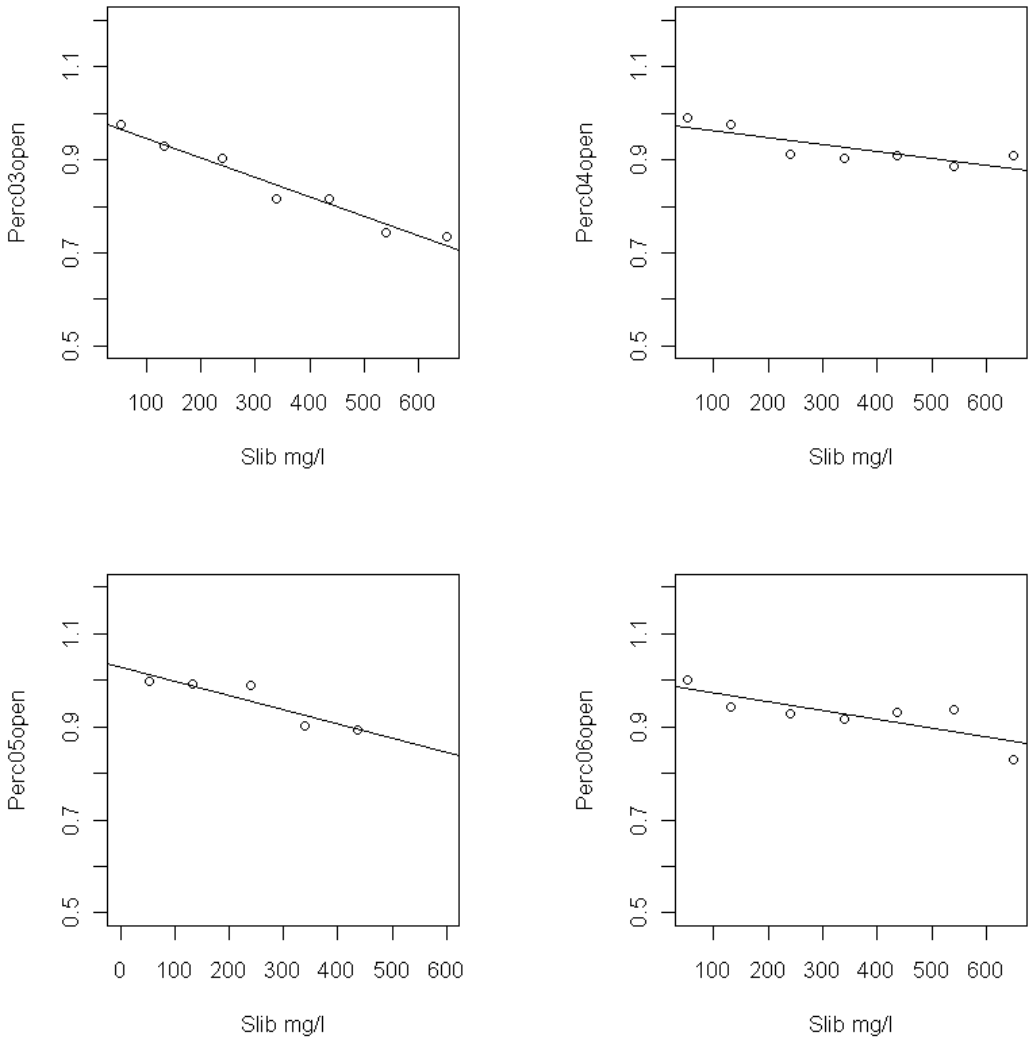

Figure 44. Figure 44. Maximum valve gape plotted against mean SPM in classes of 100 mg, All specimens dealt with above, show that their maximum valve gape decreases with increasing SPM concentrations in week 14 to 18 (April 7th-May 3rd)

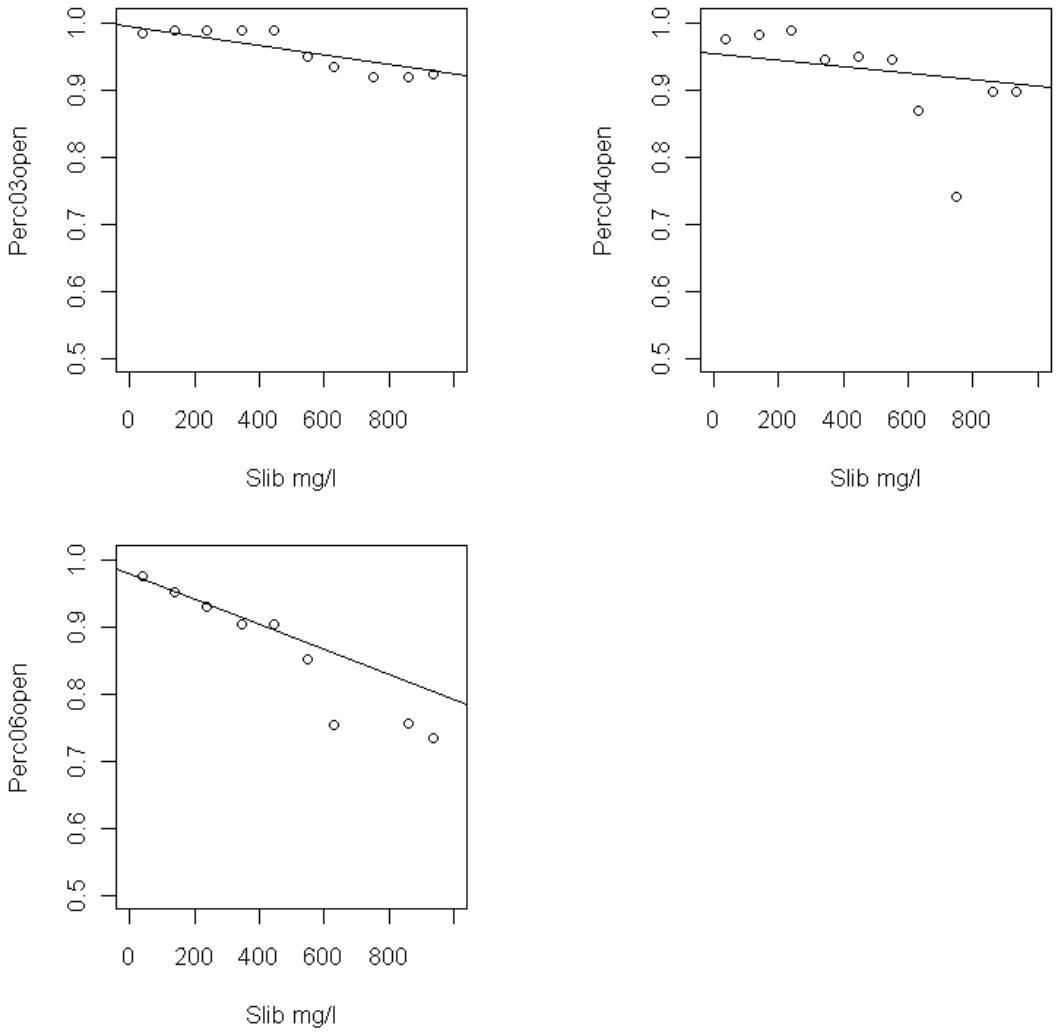

Figure 45. Maximum valve gape plotted against mean SPM in classes of 100 mg, All specimens dealt with above show that their maximum valve gape decreases with increasing SPM concentrations in week 18 to 22 (May 3rd-May 31st).

Ensis growth and Environment

The relationships between the various growth parameters as being measured for *Ensis* and the average environmental conditions measured in the period preceding the sampling date is based on the size measurements averaged over all four stations (LNE,LNW,LSW,LSE). The four stations are so close to the lander that in respect to watermovement local differences in food availability or quality are unlikely to be the underlying reason for the observed size differences. And in case there exist local food differences on that scale, the single spot measurement at the lander location could never be regarded as representative for the four separate locations. Figure 16 suggests that the growth of soft tissue and shell carbonate growth are misaligned in time. In Figure 46, 47 and 48 shell growth, condition index and percentage of gonad mass are plotted against those environmental factors which are regarded as factors which might control shell- and tissue growth.

Whereas shell growth does not start before early summer (Fig 46), tissue growth expressed as an positive change in the condition index (Fig 47) takes place in spring. The increase in condition index is accompanied with an increasing percentage of gonad tissue up to the beginning of May

(Fig 48). Latter figure also suggests that in 2011 a large spawning event took place in May at the end of the spring bloom as illustrated by the decrease in gonadal mass.
Comparison of the timing of shell growth and the change in condition index shows shell lengths start to increase once the condition index is maximal after the spawning event. Suggesting that the animals need a recovery period after spawning before energy can be spend to shell growth.

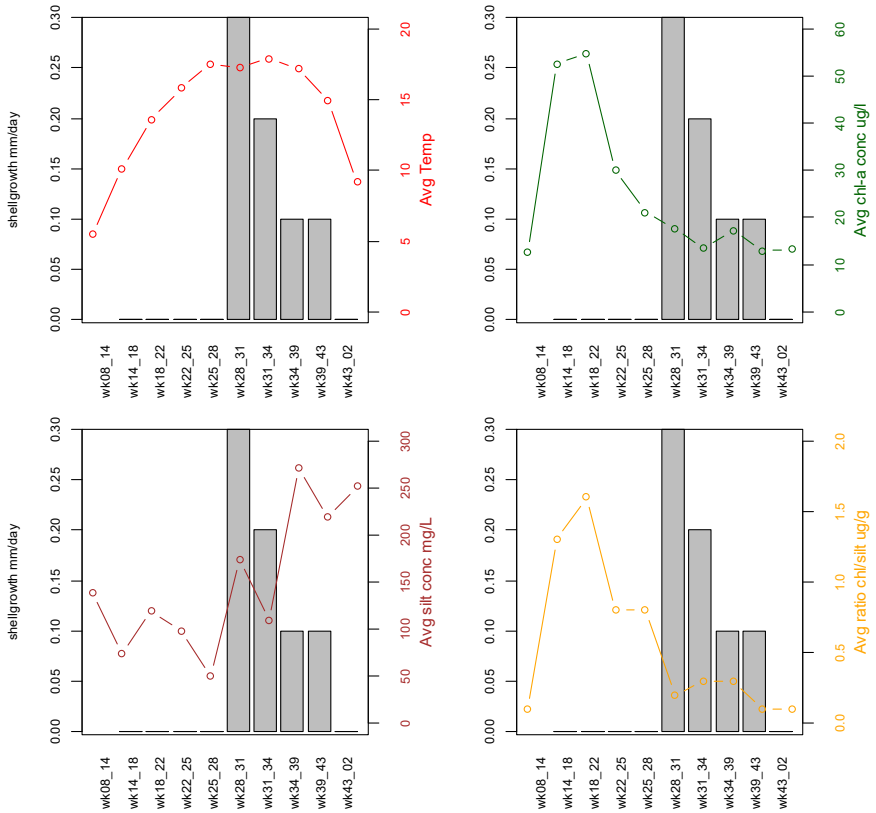

Figure 46. Shell growth (mm/day) plotted between measurement periods together with the average values of the main environmental variables, i.e. Temperature, Chlorophyll concentration, Silt concentration and the quality of the potential food source expressed as ratio between chlorophyll and silt. The data suggest that shell growth does not take place before temperatures of approximately 15 °C have been reached. Anyhow, long after the spring bloom has passed.

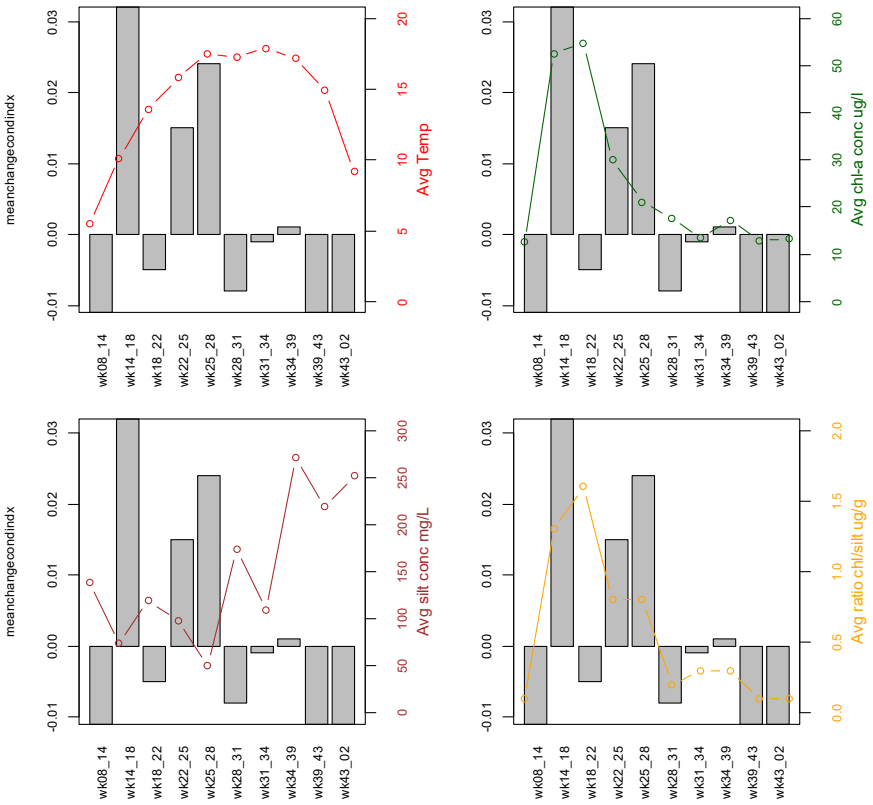

Figure 47. Change of the mean condition index between measurement periods together with the average values of the main environmental variables, i.e. Temperature, Chlorophyll concentration, Silt concentration and the quality of the potential foodsource expressed as ratio between chlorophyll and silt. The data suggest that the soft tissue mass increases in spring coinciding with the springbloom and the availability of high quality food.

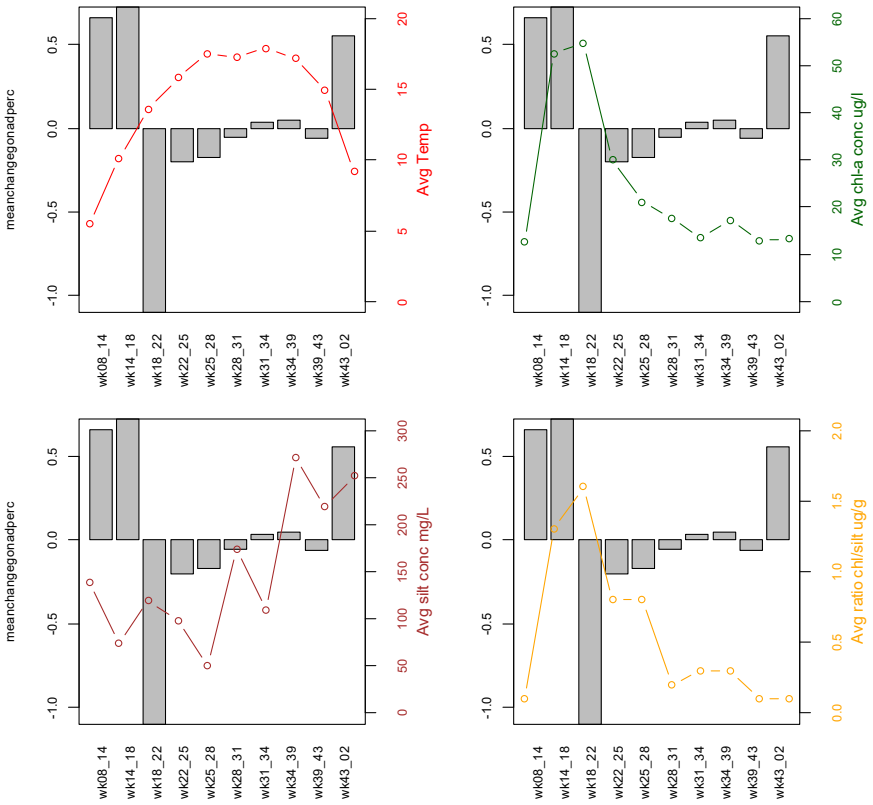

Figure 48. Change of the percentage of gonadal tissue between measurement periods together with the average values of the main environmental variables over these periods, i.e. Temperature, Chlorophyll concentration, Silt concentration and the quality of the potential foodsource expressed as ratio between chlorophyll and silt. The data shows a decrease in gonadal tissue mass in may during the end of the spring bloom.

4. Preliminary conclusions.

- The data analyzed so far illustrate that there is a marked seasonal variation in the concentrations of chlorophyll and suspended particulate matter. Peak concentrations of SPM at 30 cm above the bottom exceed 2500 mg/L during storm events. Such events have been observed to occur throughout the year. Chlorophyll peak concentrations are mainly linked to the spring phytoplanton bloom.
- The measurement of SPM at four heights close to the bottom suggests that a “blanket” of suspended material is present. The dynamics and composition of this blanket appears to be moderated by the seasonal variations in primary production and hydrodynamics.
- Tidal and wind induced currents and waves cause resuspension and mixing of organic and inorganic light particles. The spring phytoplankton bloom causes a large seasonal difference in the quality of the available near bottom food.
- Variations in the levels of suspended mud over the year show that these variations are mainly controlled by wind induced waves and currents.
- Measurement taken during ongoing beach nourishments in June 2011 suggest that under the then prevailing weather conditions the supposed increase of suspended inorganic material is small when compared to storm events later in the year.
- The data illustrate that the spring bloom in April and May temporarily changes the characteristics of the resuspended material.
- Data on the valve movements of *Ensis* under varying mud concentrations suggests that maximum valve opening decreases with increasing mud concentrations. As such the results corroborate lab experiments at which decreasing clearance rates were found at increasing clay particle concentrations.
- The data suggest that *Ensis directus* utilizes the spring related increase in food quality, expressed as ratio between chlorophyll and mud mainly for soft tissue growth and gonadal development. The main spawning of *Ensis* in 2011 took place at or shortly after the spring bloom.
- The changes in average population shell size suggest that shell growth starts half way the summer at water temperatures above 15°C.

Addendum; Data integrity.

The location where the lander platform has been deployed is a site which is about 1 km off shore at a water depth of 11 meter. Apart from human activities such as fisheries and recreation, extreme wave heights and current speeds and associated sediment scour and sedimentation might seriously impose negative effects on the integrety of the data. These problems have an stochastic character, while the problem of overgrowth by sessile organisms such as barnacles, hydrozoa and sedimentation of large amounts of SPM have a more seasonal character.
In the selection of the instruments used for this project, in combination with the tight maintenance schedule and prophylactic measures we managed to minimise the loss of data due to fouling.
The Turbidity and Fluoresence measures have been made with the wiped version of the JFE – ALEC data loggers. The wiper appeared to be a sufficient means to keep fouling under control (Figure 49)

Figure 49. Overgrown Alec Turbidity sensor. The wiped area is perfectly clean while the surrounding area is heavily over grown by barnacles.

The CTD we used is a pumped version and the pumped interior is protected from fouling by a TBT resin tablet, preventing overgrowth of fouling organisms in the flow circuit and on the sensors.
Both Nortek current meters work acoustically. The acoustic screens are protected by a veneer of udder ointment, preventing fouling, without influencing the sensitivity of the acoustic signal. The pressure sensor might however suffer from ongrowth/ingrowth of epifauna as well, resulting in a gradually change of the pressure signal.

One of the aspects which is hard to control are the physical conditions. In some periods, effects of sediment scour, high currents and waves got “grip” on the lander platform, resulting in movements and replacement. At the end of the winter period (January 11th) the lander platform had moved 150 meter to the south in relation to its deployment position.
Both the Nortek current meters, log such movements by storing “Heading”, “Tilt” and “Roll”. From these records insight into the occurrence of potential measurement errors can be obtained. Errors themselves are also given in special error and status messages stored with the data. From these messages the times at which the data are suspect can be determined. In Figure 50 a time record with of such measurement errors, as being logged by the Vektor currentmeters, is

given. The green line gives the period of the year in which fouling potentially can have had an influence on the obtained data quality. The red, vertical bars/spikes give the times/dates that the current meter data are known to be unreliable. The observed errordays in July probably deal with disturbance caused by fishing. The other spikes/bars in the record are related to bad weather. Serious bad weather started on December 7th . At that moment also a (linked?) clock error of the vektor current meter occurred, i.e. the instrument clock was not in line more with actual time. The observed time difference at the end of this measurement period is used to realign the measurements with a linear interpolation of time over the measurement bursts. A comparison between the pressure data from the ctd and the vektor currentmeter showed that up to December 7th time allignment was right.

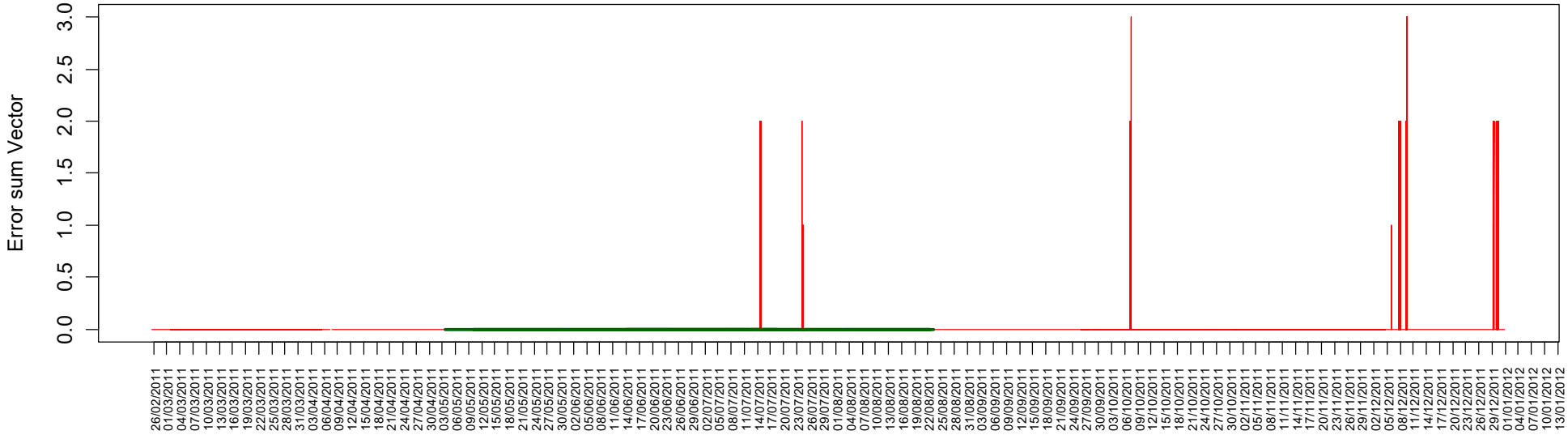

Figure 50. Fouling record of the lander and error record of the Nortek Vektor current meter. The green horizontal bar indicates the period in which significant fouling (mainly barnacles) was present. The red spikes indicate cumulative recorded measurement errors of the Vektor current meter. At the spike times, tilt, Roll and Heading changed beyond the levels that measurements were reliable. Over the 11 month measurement period there were 5 moments at which the errors indicate that the data are unreliable.

REFERENCES

Anonymous, 2002. Noordzee-atlas voor zwevend stof op basis van satellietbeelden in 2000. Rapport RIKZ/IT/2002.102: 33pp.

Alphen van, J.S.L.J. (1990) A mud balance for the Belgian-Dutch coastal waters between 1969 and 1986. Neth. J. Sea Research 25, 19-30.

Archambault M.-C, Bricelj V.M., Grant J., Anderson D.M., 2004. Effects of suspended and sedimented clays on juvenile hard clams, *Mercenaria mercenaria*, within the context of harmful algal bloom mitigation. Marine Biology 144: 553-565.

Cardoso J.F.M.F, Nieuwland G., Wijsman J., Witbaard R., Van der Veer H.W., 2011. Validation of a method for age determination in the razor clam *Ensis directus*, with a review on available data on growth, reproduction and physiology. NIOZ-Report 2011-9: 33 pp.

Cardoso, J.F.M.F.,H,W. van der Veer, S.A.L.M. Kooijman, 2006. Body-size scaling relationships in bivalve species: A comparison of field data with predictions by the Dynamic Energy Budget (DEB) theory. Journ. Sea Res, 56(2):125-139.

Cardoso, J.F.M.F, Witte, IJ, Veer van der, H.W., 2009. Reproductive investment of the American razor clam *Ensis americanus* in the Dutch Wadden Sea. Journal of Sea Research, 62 (4) 295–298.

Duin C.F. van Gotjé ,W., Jaspers C.J. & Kreft M., 2007. MER Winning suppletiezand Noordzee 2008 t/m 2012. Grontmij Hoofdrapport, Definitief. 13/99080995/CD, revisie D1 242 pp, Grontmij, Houten.

Ellerbroek, G., M.J.C. Rozemeijer, J.M. de Kok, J. de Ronde, 2008. Monitoring and Evaluation Programme Sand mining RWS LaMER, part B5 of the evaluation programme Sand mining. Ministerie van verkeer en waterstaat, Noord holland.

Kok,de J. M., 2004. Slibtransport langs de Nederlandse kust. Bronnen, fluxen en concentraties. Rapport RIKZ/OS/2004.148w: 31pp.

Goudswaard, P.C.; Kesteloo, J.J.; Perdon, K.J.; Jansen, J.M., 2008.
Mesheften (*Ensis directus*), halfgeknotte strandschelpen (*Spisula subtruncata*), kokkels (*Cerastoderma edule*) en otterschelpen (*Lutraria lutraria*) in de Nederlandse kustwateren in 2008. Yerseke : IMARES, (Rapport / IMARES C069/08)

Goudswaard P.C., K.J. Perdon, J.Jol, J.J. Kesteloo, C. van Zweeden & K. Troost, 2011. Schelpdieren in de Nederlandse kustwateren Bestandsopname 2011. Imares rapport c094/11 78pp.

Kamermans, P., Brummelhuis, E. & Wijsman, J., 2011. First pioneering laboratory experiments on filtration, respiration and growth of the razor clam (*Ensis directus*, Conrad) IMARES Rapport C115/11, 48pp.

Schellekens, T. 2012. Groei en conditie van zwaardschede (*Ensis directus*, Conrad) Imares concept rapport 2012, 29pp.

Wilber D.H., Clarke D.G., Rees S.I., 2007. Responses of benthic macroinvertebrates to thin-layer disposal of dredged material in Mississippi Sound, USA. Marine Pollution Bulletin 54: 42-52.

Wijsman, J.W.M.,2011. Dynamic Energy Budget (DEB) parameters for *Ensis directus.* Yerseke: IMARES, (Report C116/11). 39pp.

Witbaard, R. & P. Kamermans, 2011. De bruikbaarheid van de klepstandmonitor op *Ensis directus* ten behoeve van de monitoring van aan zandwinning gerelateerde effecten.NIOZ rapport 2009-10, 44 pp

Het NIOZ Koninklijk Nederlands Instituut voor Zeeonderzoek is een instituut van de Nederlandse Organisatie voor Wetenschappelijk Onderzoek (NWO).

Bezoekadres
Landsdiep 4
1797 SZ 't Horntje, Texel

Postadres
Postbus 59, 1790 AB Den Burg, Texel
Telefoon: 0222 - 369300
Fax: 0222 - 319674
http://www.nioz.nl

NIOZ Rapport 2012-7

De missie van het NIOZ is het verkrijgen en communiceren van wetenschappelijke kennis van zeeën en oceanen voor een beter begrip en een duurzaam beheer van onze planeet, het beheren van de nationale faciliteiten voor zeeonderzoek en het ondersteunen van onderzoek en onderwijs in Nederland en in Europa.